Magnetic Resonance Imaging of Cartilage Repair: A Review

Siegfried Trattnig[1], Carl S. Winalski[2], Stephan Marlovits[3],
Jukka S. Jurvelin[4], Goetz H. Welsch[1,5], and Hollis G. Potter[6]

Abstract

Articular cartilage lesions are a common pathology of the knee joint, and many patients may benefit from cartilage repair surgeries that offer the chance to avoid the development of osteoarthritis or delay its progression. Cartilage repair surgery, no matter the technique, requires a noninvasive, standardized, and high-quality longitudinal method to assess the structure of the repair tissue. This goal is best fulfilled by magnetic resonance imaging (MRI). The present article provides an overview of the current state of the art of MRI of cartilage repair. In the first 2 sections, preclinical and clinical MRI of cartilage repair tissue are described with a focus on morphological depiction of cartilage and the use of functional (biochemical) MR methodologies for the visualization of the ultrastructure of cartilage repair. In the third section, a short overview is provided on the regulatory issues of the United States Food and Drug Administration (FDA) and the European Medicines Agency (EMEA) regarding MR follow-up studies of patients after cartilage repair surgeries.

Keywords

magnetic resonance imaging, knee, articular cartilage, glycosaminoglycans, cartilage repair

Part 1: Preclinical Models

Basic Requirements

The challenges of using preclinical models include the smaller tissue dimensions compared with humans and species-specific differences in joint morphology. These factors can make it difficult or impractical to image using some standard radiofrequency (RF) coils that have been optimized for clinical imaging. Imaging of specimens requires careful preparation. The animal limb may not fit the geometry of the coil, and with intact joints, a posterior soft tissue release of the capsule or posterior tendons of the specimen or stifle may be necessary in order to obtain sufficient limb extension to fit into a clinical extremity or wrist coil. In the setting of cartilage repair, caution should be utilized so as not to incise the capsule and thereby introduce air pockets that may create susceptibility artifact and hamper both morphological and, in particular, quantitative magnetic resonance (MR) assessment. Alternatively, RF coils may be built or custom ordered. Imaging of excised specimens *ex vivo* offers the opportunity to use small bore magnets and coils that can provide better signal-to-noise ratios (SNRs) and potentially higher spatial resolution.

MR evaluation may include both high-resolution morphological assessment of the cartilage as well as quantitative MR techniques aimed at selectively targeting both proteoglycan and collagen. High-resolution imaging is recommended in order to assess subtle fissures developing at the area of peripheral integration as well as development of proud subchondral bone formation that may be seen following marrow stimulation repair techniques. Spatial resolution should ideally be less than 200 μm in the frequency and preferably in the phase direction, with thin slice resolution of 1 to 2 mm or less. In order to maintain an adequate SNR, imaging at field strengths higher than 1.5 T is generally recommended.

Institution where the research was conducted: MR Centre - High Field MR, Department of Radiology, Medical University of Vienna, Vienna, Austria.

[1]MR Centre - High Field MR, Department of Radiology, Medical University of Vienna, Vienna, Austria
[2]Cleveland Clinic Foundation, Cleveland, OH, USA
[3]Trauma Surgery Department, Medical University of Vienna, Vienna, Austria
[4]Department of Physics and Mathematics, University of Eastern Finland, Kuopio, Finland
[5]Department of Trauma Surgery, University Hospital of Erlangen, Erlangen, Germany
[6]Hospital for Special Surgery, MRI, New York, NY, USA

Corresponding Author:
Siegfried Trattnig, MR Centre - High Field MR, Department of Radiology, Medical University of Vienna, Lazarettgasse 14, A-1090 Vienna, Austria
Email: siegfried.trattnig@meduniwien.ac.at

It is further recommended that imaging time points be applied to preclinical models that reproduce or can help choose the appropriate time points to be used in the preliminary (phase I) clinical trial. This will allow for the longitudinal assessment of the biological behavior of the repair and/or implant by obtaining morphological and quantitative MR imaging (MRI) data at different time intervals following the surgery before application to a clinical trial. Variables such as advancement of the subchondral bone plate, osteolysis surrounding bioabsorbable devices or scaffolds, inflammatory adverse synovial reaction, and the presence or absence of stratification of the repair tissue on quantitative MR should be measured. Correlation between MRI and histology can provide valuable information that may help with the interpretation of patient images obtained in future clinical trials; that is, particular measures on qualitative or quantitative MRI may prove specific to certain histological findings.

Use of Contrast Agents

MR contrast agents have been used for imaging of native articular cartilage or cartilage repair tissue either to delineate the articular surface (arthrography) for the detection of defects or to measure the biochemical status of the articular cartilage (delayed gadolinium-enhanced MRI of cartilage [dGEMRIC]). The most commonly used MR contrast agents are gadolinium (Gd) chelates. A variety of these agents are commercially available. Most of the compounds are nonionic; only gadopentetate dimeglumine (Gd-DTPA), available as Magnevist (Bayer HealthCare, Leverkusen, Germany), has a charge (2−). While any of the Gd chelates may be used for arthrography, only Gd-DTPA is suitable for mapping of the proteoglycans with dGEMRIC because of its molecular charge. *Ex vivo*, arthrography and dGEMRIC must be performed either with a direct intra-articular contrast injection, if the joint is intact, or the desired articular surface may be dissected and placed in a contrast agent bath during imaging or for equilibration prior to imaging (dGEMRIC).

Most Gd-chelate MR contrast agents are small and readily diffuse into articular cartilage.[1] The diffusion of MR contrast agents into cartilage and cartilage repair tissues is a time-dependent phenomenon. A concentration gradient initially forms with higher concentration closer to the source of the contrast agent (cartilage interface). For intra-articular fluid injection or submersion in a fluid bath, the contrast diffuses from the articular surface into the deep tissue. Following intravenous injection (*in vivo*), the contrast will diffuse into the articular cartilage from both the joint fluid and the subchondral bone.[2] The time to achieve equilibrium will vary by the square of the thickness of the articular cartilage or the repair tissue; that is, cartilage that

is twice as thick will take 4 times as long to equilibrate. For *ex vivo* samples, true equilibration of the contrast agent concentration between the tissue and fluid can be achieved. However, *in vivo*, the concentrations within vasculature, synovium, joint fluid, subchondral bone, and cartilage are varying with time, and only a "dynamic" equilibrium can be achieved.

When performing dGEMRIC experiments, the thickness of the cartilage or repair tissue and the route of contrast administration must be considered when planning the time that will be required for full penetration of the cartilage. With deep lesions, thick cartilage, or thick repair tissue, the time to contrast equilibration within the tissues may be prohibitively long. Recently, Dugar et al. found that dGEMRIC of articular cartilage may be performed *ex vivo* following fixation in paraformaldehyde.[3] To our knowledge, however, postfixation dGEMRIC has not been validated for cartilage repair tissues.

For calculations of fixed charge density (FCD) and proteoglycan content using dGEMRIC, the precontrast and postcontrast T1 values for articular cartilage are required as well as the concentration of Gd-DTPA in the joint fluid or fluid bath.[2] Because the T1 of unenhanced native articular cartilage is relatively constant, it has been suggested that the dGEMRIC protocol be streamlined by estimating FCD without obtaining precontrast images.[4] However, some authors have shown differences between the precontrast T1 values of autologous chondrocyte implantation repair tissue and articular cartilage, and therefore, obtaining only postcontrast T1 measurements for dGEMRIC may lead to erroneous conclusions about the relative FCDs of the tissues.[5] For the study of cartilage repair tissues, it is recommended that precontrast and postcontrast T1 measurements be obtained when possible. If this is not feasible, determination of unenhanced T1 values for the type and stage of maturity of the repair tissue should be performed to confirm that a consistent T1 value within the repair tissues may be assumed for FCD estimations. When performing MR arthrography for articular surface evaluation with either intra-articular injection or specimen immersion in a contrast agent bath, imaging shortly after contrast administration is desirable to maximize the image contrast between the cartilage and fluid.

Functional, Biomechanical MRI of Repair Tissue

Articular cartilage is structurally multiphasic, inhomogeneous, mechanically anisotropic, and nonlinear. Mechanical properties of articular cartilage are determined by the content, arrangement, and interactions of the tissue constituents, that is, 3-dimensional (3-D) collagen network, proteoglycans (PGs), and interstitial water.[6] This structural interplay creates a poroviscoelastic tissue response to

mechanical loads on the joint.[7] PGs and collagen have been shown to be primary determinants of compressive and tensile properties of cartilage, respectively. Further, the collagen fibrils strongly contribute to the compressive response under dynamic and impact loading of cartilage.[8]

MRI can provide information on cartilage morphology, intrinsic composition, and structure. Although no MRI parameter may be fully specific to any tissue component, quantitative parameters have been related to tissue biomechanical properties. Further, it has been proposed that MRI could serve as a surrogate marker for cartilage biomechanical properties. Because of the complexity of cartilage mechanical characteristics, individual quantitative MRI parameters can characterize only limited features of cartilage biomechanics. In several *in vitro* studies, dGEMRIC (or $T1_{Gd}$), by providing information on tissue PG content, has been related to PG-sensitive mechanical parameters, especially to the compressive modulus of tissue.[9-11] However, the strength of the dGEMRIC-equilibrium modulus association has been variable, obviously depending on the homogeneity of the sample material. For example, when *in vitro* samples are taken from native and repaired tissues, overall cartilage structure may vary significantly and lead to major differences in mechanical modulus that cannot be explained by the variations in PG content of samples, and in this case, the correlation is low.[12] Biomechanical properties of the repair tissue may remain inferior, even though in some cases, the tissue stiffness can reach 90% of that in healthy tissue.[13,14] Interestingly, the repair tissue at 12 months after autologous chondrocyte implantation (ACI), showing highly replenished PG content by dGEMRIC, demonstrated an inferior compressive stiffness, as assessed by the indentation technique.[15] This implies that the functional integrity of the repair tissue has been inferior, likely due to the disorganized 3-D matrix structure.

T2 values have been related to both water[16,17] and collagen[18] content of cartilage but especially to collagen network structure.[19] Experimental tissue degeneration by enzymatic digestion of the tissue collagen network increased T2 values. However, enzymatic depletion of PGs had no significant effect on T2.[20] In both cases, the mechanical stiffness of cartilage was significantly reduced. The strength of the correlation between T2 values and tissue mechanical characteristics has proved variable. Because the spatial T2 closely follows the depth-wise architecture of the collagen network, the bulk values may not be indicative of tissue integrity, and T2 does not appear to be a definitive indicator of cartilage stiffness. In previous cartilage repair studies, T2 values of repair tissue at early postoperative time points reveal depth profiles different than native tissue and were typically higher in repair tissue than in native tissue.[21,22] However, at 19 to 24 months after the matrix-associated autologous cartilage transplantation, tissue T2 profiles

were more normalized.[22] Based on these results, $T1_{Gd}$ and T2 combined could bring complementary information of engineered cartilage and enable more comprehensive characterization of the mechanical competence of repair tissue.

The limitation of MRI is its inability to directly quantify functional properties of cartilage or repair tissue. In order to extract direct information on tissue biomechanics, mapping of the intrinsic deformation under experimental loading during MRI by using elastographic techniques[23,24] has been used to describe tissue mechanical function. For *in vivo* analysis of repair tissue function, limited MRI resolution for small repair lesions, as well as technical arrangements for *in vivo* loading during MRI scanning, are challenging. As an alternative, using quantitative MRI information, numerical models have been developed to predict mechanical behavior of cartilage tissue and even to extract values of mechanical properties without mechanical testing.[25,26] In this functional imaging approach, the joint geometry, cartilage composition, and structure from the MRI are incorporated into a finite element model; tissue function is predicted, and changes in tissue architecture in loaded articular cartilage are estimated. Using the fibril-reinforced poroelastic model of cartilage, it has been found that the collagen and PG-specific MRI parameters correlated significantly with the corresponding mechanical parameters of articular cartilage, that is, the fibril network modulus (collagen) and the nonfibrillar matrix modulus (PGs).[27] The first studies suggest that functional imaging with accurate joint geometry from MRI may enable large-scale 3-D simulations of joint loading.[26] Importantly, patient-specific models and diagnostics of the cartilage mechanics, including repair tissue analysis, may be feasible.

Part 2: Clinical Studies
Morphological MRI Studies

Basic MR Technical Requirements

Native articular cartilage and postoperative cartilage repair tissue are relatively thin structures that cover curved surfaces and thus require high-quality, high-resolution images for accurate assessment. As with all imaging technologies, with MRI, there is always a trade-off between the image SNR, spatial resolution, and image acquisition time. The following equation demonstrates some of the relationships between SNR and imaging parameters:

$$SNR \propto Pix_{area} \bullet SliceThickness \bullet \sqrt{\frac{\# Excitations}{Bandwidth}},$$

where "Pix_{area}" is the area of an image pixel within the slice, "SliceThickness" is the thickness of the image slice, "# Excitations" is the number of spatial encoding steps times

the number of averages used in the acquisition, and "Bandwidth" is the bandwidth of the signal receiver. The pixel area and slice thickness determine the spatial resolution (voxel volume) of the image, while the number of excitations is a major determinant of the acquisition time. Acquisition time is linearly proportional to the number of excitations; for example, a doubling in spatial encoding steps or number of averages will double the acquisition time. From this relationship, improvement of the spatial resolution with a 2-fold decrease in each of the in-plane pixel dimensions (e.g., 0.3 mm × 0.3 mm rather than 0.6 mm × 0.6 mm) will result in a 4-fold decrease in SNR for the same slice thickness and with all other parameters remaining constant. To achieve the same SNR for the higher resolution scan, a 16-fold increase in the number of excitations would be required. This 16-fold increase in imaging time may not be clinically acceptable. Because it is difficult to achieve the image resolution required for cartilage repair assessment solely by increasing the imaging time of an acquisition, optimization of the imaging equipment is essential.

The magnet determines the imaging field strength, which greatly influences the SNR of the system. If all other components are kept constant (which is usually not possible), the SNR of the MR system varies in direct linear proportion to the magnetic field strength. Thus, a 3-T magnet system has the potential to double the SNR of a 1.5-T system and has 15 times the SNR of a 0.2-T system. Therefore, use of high-field (≥1.5 T) MR systems is recommended for imaging of articular cartilage repair tissue.

The MRI of cartilage repair can be obtained at most clinically available MR systems. Although the depiction of the cartilage repair tissue, the adjacent cartilage, and the surrounding structures can be achieved without high resolution, it has been demonstrated that a voxel size under 300 µm is required to reveal fraying of the articular surface of cartilage.[28] High-field MRI units with 1.5 T and especially 3.0 T have provided the means to achieve such resolution in reasonable scan times while using cartilage-sensitive sequences. To further decrease the scan time while maintaining high-resolution parameters, dedicated coil technology with multielement design enables the use of parallel imaging. This technology can decrease scan time by a factor of 2 to 3 with a 3.0-T MR scanner, despite the inherent loss in SNR. High-field MRI also permits the use of 3-D acquisitions that yield high resolution, high SNR, and high contrast-to-noise ratios (CNRs). Furthermore, isotropic MRI, that is, acquisitions with voxel dimensions that are equal in all 3 axes, allows for multiplanar reconstruction (MPR) in any plane without any loss of resolution.[29-31]

Cartilage-Specific Sequences

Standard morphological MR evaluation of cartilage repair tissue can be performed using the same acquisition

Figure 1. Conventional axial proton density fast spin-echo (PD FSE) sequence (TR/TE: 2400/28) with ultra-high resolution (512 × 512; 12 cm; slice thickness: 2 mm) of a 17-year-old male patient 3 months after matrix-associated autologous chondrocyte transplantation (MACT) of the patella. The double-layered scaffold is still visible.

techniques as those used for native cartilage.[32] The most widely used MRI techniques are intermediate-weighted fast spin-echo (FSE) and 3-D fat-suppressed T1-weighted gradient-echo (GRE) acquisition.[29,30,32-34] Whereas the GRE sequence visualizes cartilage defects attributable to T1 differences between cartilage and fluid, the FSE sequence uses differences in T2 weighting. Compared with fluid, cartilage is higher in signal intensity on fat-suppressed T1 weighting and lower on intermediate or T2 weighting. While the T1-weighted, 3-D GRE sequence with fat suppression is suitable for visualization of the thickness and surface of cartilage and allows 3-D volume measurements, the FSE sequence is more sensitive for assessment of the internal cartilage structure.[29,32,33] In postoperative imaging, one advantage of FSE sequences is its low sensitivity to artifacts, which are suppressed by the 180° refocusing pulses of the FSE (**Fig. 1**). Both sequences, the fat-suppressed, 3-D GRE and the FSE, are showing excellent results with high sensitivity, specificity, and accuracy for detecting cartilage lesions in the knee.[29,32,35]

Currently, isotropic 3-D sequences have the potential of high-resolution imaging with a voxel dimension as small as 0.4 mm^3 and can be reformatted in any plane. These acquisitions may be gradient echo based, including SPGR (spoiled gradient echo), FLASH (fast-low angle shot), VIBE (volume-interpolated breath-hold examination), DESS (double-echo steady state), SSFP (steady-state free
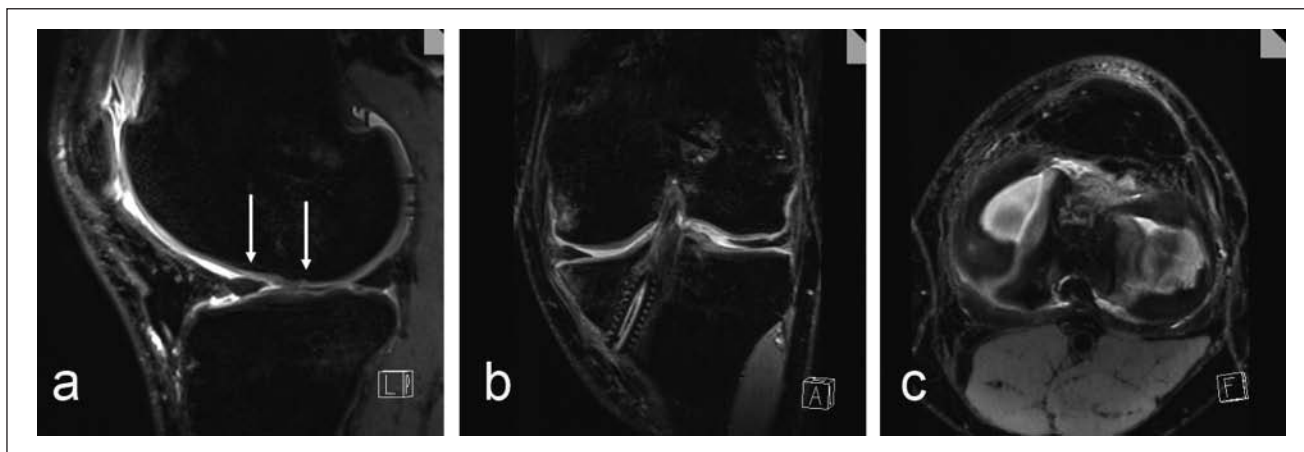
Figure 2. High-resolution, isotropic, 0.5 × 0.5 × 0.5-mm fat-suppressed 3-D proton density (PD) SPACE sequence (TR/TE: 1500/34) to assess postoperatively the cartilage repair tissue 6 months after microfracture (arrows, sagittal) (**a**), the position and orientation after anterior cruciate ligament surgery (coronal) (**b**), and the menisci (axial) (**c**) in a 30-year-old male patient using multiplanar angulated reconstruction from one isotropic data set.

precession), True-FISP (fast imaging with steady-state precession), or more recently developed FSE sequences, called SPACE (sampling perfection with application-optimized contrasts using different flip-angle evolutions), 3-D Fast Spin-Echo Extended Echo Train Acquisition (FSE-XETA, also known as 3-D FSE-CUBE), or VISTA, which may, contingent on validation studies, provide accurate evaluation of cartilage and cartilage repair tissue as well as the other joint structures, especially in postoperative imaging.

One of the most often used isotropic 3-D sequences for cartilage imaging is the FLASH sequence, a fat-suppressed, T1-weighted, gradient-recalled echo sequence with RF spoiling.[31] The fat-suppressed, 3-D FLASH sequence shows high CNRs and high reproducibility in the segmentation of articular cartilage, which facilitates accurate evaluation of total cartilage volume and regional distribution.[36,37] Quantitative MR cartilage segmentation measurements including cartilage thickness and volume have been suggested as sensitive image-based parameters for detecting and monitoring cartilage degeneration in osteoarthritis.[38] The 3-D DESS sequence was introduced for cartilage imaging many years ago[39] but only recently, with improved magnet systems, proved adequate to measure changes of cartilage thickness and volume in the longitudinal studies.[40] The 3-D True-FISP sequence has also been shown useful for quantitative cartilage MR with the advantage of substantially higher SNR and CNR compared with the 3-D FLASH sequence.[41] In recent articles by Duc et al.,[42-44] the True-FISP sequence, as an SSFP-based sequence, was studied in detail at 1.5 T, and using a dedicated 8-channel knee coil, isotropic (0.6 mm^3) 3-D True-FISP acquisitions were obtained in approximately 3 minutes. They found performance in diagnosing cartilage defects, anterior cruciate

ligament abnormalities, and meniscal tears comparable with a set of standard 2-D sequences.[43] However, because of artifacts, this acquisition technique may nevertheless be of limited value for postoperative imaging following cartilage repair procedures.[45]

3-D FSE sequences have also shown promising results in the assessment of cartilage lesions together with other internal knee derangements. In a comparison to 2-D FSE sequences, an isotropic (0.7 mm^3) 3-D FSE-XETA could be reformatted in arbitrary planes with high-cartilage SNR.[46] Another study found the related sequence, 3-D FSE-CUBE, to be more sensitive, but less specific, than standard 2-D acquisitions for the diagnosis of cartilage lesions.[47] Although the use of isotropic 3-D sequences for cartilage volume and thickness measurements in the follow-up evaluation of cartilage repair procedures remains challenging, there is great potential of improved 3-D assessment of the cartilage repair tissue because of the lower sensitivity to postoperative magnetic susceptibility changes. Using image post-processing viewing tools that provide MPRs, the interfaces of the cartilage repair tissue with native cartilage, subchondral bone, and joint fluid can be precisely evaluated in every plane, independent of its location within the joint (**Fig. 2**).

MR arthrography. MR arthrography generally refers to imaging of a joint following joint fluid enhancement by the contrast agent, which can be achieved either by a direct intra-articular injection or indirectly with an intravenous (IV) injection. Following IV injection, the contrast agent diffuses through the synovium into the pre-existing joint fluid, producing an "indirect" arthrogram.[48] As shown clinically, the joint fluid enhancement may be maximized by moving the joint immediately after IV injection so that all

of the joint fluid is equilibrated with the vasculature, while there is a high intravascular concentration. A delay of 15 minutes or more is recommended in human knees to maximize joint fluid enhancement for arthrography.[48,49] A longer delay is required for dGEMRIC (see below).[4] Direct and indirect MR arthrography may prove useful in assessing defects at graft/host bone following osteochondral repairs and the cartilage interface after all types of repair.

MR Classification Systems Based on Morphology

The morphology of cartilage repair tissue should be compared with the adjacent native cartilage. On MRI, the repair tissue should have a smooth articular surface that reproduces the original articular contour at the same level as adjacent native cartilage.[50] Ideally, the signal intensity of the repair tissue should be isointense to the adjacent native cartilage. To evaluate the efficacy of cartilage repair techniques in large cohorts, it is necessary to have a standardized, validated evaluation system with low interobserver and intraobserver variability that is suited for statistical data analysis. The system should have the potential to compare different cartilage surgery techniques and be applicable to multicenter studies.[51,52]

Roberts et al.[52] used 4 parameters to assess cartilage repair on MRI: surface integrity and contour, cartilage signal in the graft region, cartilage thickness, and changes in the underlying bone. A score was then obtained by summing the values of the 4 parameters. The system assessed each parameter as normal or abnormal. A more detailed classification system was proposed by Henderson et al.[53] using the parameters of defect filling (1 = complete, 2 > 50% of the defect, 3 < 50%, 4 = full-thickness defect), cartilage signal (1 = normal [identical to the adjacent articular cartilage], 2 = nearly normal [slight areas of hyperintensity], 3 = abnormal [larger areas of hyperintensity], 4 = absent), and subchondral edema and effusion (both graded as 1 = absent, 2 = mild, 3 = moderate, 4 = severe). In a separate study, Mithoefer et al.[54] assessed the "repair cartilage signal" (hyperintense, isointense, hypointense), the "repaired lesion morphology" (proud, flush, depressed), the "repair cartilage fill" (good, moderate, poor), the "peripheral repair cartilage integration" (no gap, small, large), and the "subchondral edema" (mild, moderate, severe, osseous overgrowth).

Perhaps the most complete MR evaluation is performed by the "magnetic resonance observation of cartilage repair tissue" (MOCART) scoring system.[51,55] The MOCART score claims to allow assessment of the articular cartilage repair tissue that is sensitive to subtle change. It has been used in longitudinal studies following a number of types of cartilage repair procedures.[56-75] Based on the use of MPR of an isotropic MR data set, a 3-D MOCART score has

been introduced with changes and additions based on the new information afforded by isotropic voxel MRI; clinical experiences gained from research studies; published articles, abstracts, and presentations; and on the needs of daily patient care.[45] Compared to the standard MOCART score, 3-D MOCART demonstrated a high correlation of the individual variables.[45] The 3-D MOCART score combines a descriptive part and 11 variables (**Table 1**). These variables, however, can be assessed by 3-D isotropic MRI and/or standard 2-D MR sequences; furthermore, the evaluation can be adapted to the specific needs of longitudinal MR assessment after any cartilage repair procedure in any joint. The variables are defect fill (1), cartilage interface (2), bone interface (3), surface of the repair tissue (4), structure of the repair tissue (5), signal intensity of the repair tissue (6), subchondral lamina (7), chondral osteophyte (8), bone marrow edema (9), subchondral bone (10), and effusion (11), and they are explained in detail in the article of Welsch et al.[45]

MR Findings of Following Specific Cartilage Repair Techniques

There are several established marrow stimulation techniques including abrasion arthroplasty, subchondral drilling, and microfracture. The MRI appearance of a chondral repair site treated by marrow stimulation evolves over time. In the early postoperative period, the repair site normally contains tissue that may appear thin and indistinct and with generally intermediate signal intensity. In addition, the subchondral bone marrow consistently shows features of edema-like signal intensity.[50] By 1 to 2 years after surgery, the treated defect should be filled with tissue that has a smooth, well-defined surface. In the subjacent subchondral bone of asymptomatic patients, the region of altered signal diminishes but usually does not resolve completely. By contrast, in symptomatic patients with failure of the procedure, the treated defect is incompletely filled with thinned and irregular tissue. Furthermore, the region of altered signal in the subchondral bone does not diminish; rather, it commonly becomes more conspicuous over time.[50]

Autologous osteochondral transplantation is currently considered the only surgical technique that directly provides and retains true hyaline articular cartilage. MRI following autologous osteochondral transplantation can provide information about the thickness of the cartilage cover, the congruity of the articular surface, the graft incorporation, the status of the subchondral bone, and the status of the graft donor site.[50,76] It has been shown in animal studies that the autologous osteochondral grafts usually demonstrate solid, osseous incorporation between 6 and 14 weeks.[77,78] Initially, because of the surgery itself, subchondral bone marrow edema is present and is expected

Table 1. 3-Dimensional Magnetic Resonance Observation of Cartilage Repair Tissue (3-D MOCART) Scoring

Variables	Variables
1. Defect fill (degree of defect repair and filling of the defect in relation to the adjacent cartilage) O 0 % O 0 - 25 % O 25 - 50 % O 50 - 75 % O 75 - 100 % O 100 % O 100 - 125 % O 125 - 150 % O 150 - 200 % O > 200 % Localization O Whole area of cartilage repair O > 50 % O < 50 % O Central O Peripheral O Weight-bearing O Non weight-bearing	**6. Signal intensity** (Intensity of MR signal in the repair tissue in comparison to the adjacent cartilage) O Normal (identical to adjacent cartilage) O Nearly normal (slight areas of signal alteration) O Abnormal (large areas of signal alteration) Localization O Central O Peripheral O Weight-bearing O Non weight-bearing
2. Cartilage Interface (integration with adjacent cartilage to border zone in two planes) Sagittal (Femur, Patella, Trochlea, Tibia) O Complete O Demarcating border visible (split-like) O Defect visible <50 % O Defect visible >50 % Coronal (Femur, Tibia); Axial (Patella, Trochlea) O Complete O Demarcating border visible (split-like) O Defect visible <50 % O Defect visible >50 % Localization O Whole area of cartilage repair O > 50 % O < 50 % O Weight-bearing O Non weight-bearing	**7. Subchondral lamina** (Constitution of the subchondral lamina) O Intact O Not intact Localization O Whole area of cartilage repair O > 50 % O < 50 % O Central O Peripheral O Weight-bearing O Non weight-bearing
3. Bone interface (integration of the transplant to the subchondral bone; integration of a possible periosteal flap) O Complete O Partial delamination O Complete delamination O Delamination of periosteal flap Localization O Weight-bearing O Non weight-bearing	**8. Chondral Osteophytes** (Osteophytes within the cartilage repair area) O Absent O Osteophytes < 50 % of the thickness of the cartilage transplant O Osteophytes > 50 % of the thickness of the cartilage transplant Localization Size: _____ mm (plane: _____) x _____ mm (plane: _____) O Central O Peripheral O Weight-bearing O Non weight-bearing
4. Surface (constitution of the surface of the repair tissue) O Surface intact O Surface damaged <50% of depth O Surface damaged >50% of depth O Adhesions Localization O Whole area of cartilage repair O > 50 % O < 50 % O Central O Peripheral O Weight-bearing O Non weight-bearing	**9. Bone marrow edema** (Maximum size and localization in relation to the cartilage repair tissue and other alterations assessed in the 3D MOCART score). O Absent O Small (< 1cm) O Medium (< 2cm) O Large (< 4cm) O Diffuse Localization Size: _____ mm (plane: _____) x _____ mm (plane: _____) O Central O Peripheral O Weight-bearing O Non weight-bearing O Relation to other alterations within this score of variable No. _____.
5. Structure (constitution of the repair tissue) O Homogeneous O Inhomogeneous or cleft formation Localization O Whole area of cartilage repair O > 50 % O < 50 % O Central O Peripheral O Weight-bearing O Non weight-bearing	**10. Subchondral bone** (Constitution of the subchondral bone) O Intact O Granulation tissue O Cyst O Sclerosis Localization O Whole area of cartilage repair O > 50 % O < 50 % O Central O Peripheral O Weight-bearing O Non weight-bearing
	11. Effusion (Approx. size of joint effusion visualized in all planes) O Absent O Small O Medium O Large

Variables 1-11 for 3D MOCART score; subcategories "localization" optional.

to resolve as the graft incorporates into the subchondral bone. Normal, fatty marrow signal is usually seen within and around the plugs when solid bony incorporation occurs. Poor integration of the graft may be suggested when MRI shows cystic cavities with fluid-like signal intensity and persistent edema-like signal within the subchondral bone marrow.[79]

Following ACI, MRI can help define the defect fill, the integration of the graft with the underlying bone and adjacent native cartilage, and the status of the subchondral bone plate and bone marrow.[50] At most ACI sites, the chondral defect is completely filled with the repair tissue to the expected level of the adjacent articular cartilage.[50] In cases of incomplete defect fill, MR can demonstrate underfilling of the repair site either in focal areas or as an overall thin cartilage.[50] Graft failure through delamination has been reported to occur in approximately 5% of patients and usually presents within the first 6 postoperative months.[80] The interface between an ACI and native cartilage may be indiscernible or appear as a sharp line. In ACI procedures, the term "partial delamination" is used for incomplete integration of the repair tissue (**Fig. 3**).[50] A common complication after ACI is hypertrophy of the periosteal cover, which often occurs between the third and ninth postoperative months and has been reported in up to 20% to 25% of ACI patients.[81] On MRI, periosteal hypertrophy results in a graft

Figure 3. Conventional sagittal proton density fast spin-echo (PD FSE) sequence (TR/TE: 2400/28) with ultra-high resolution (512 × 512; 12 cm; slice thickness: 2 mm) of a 28-year-old male patient 24 months after matrix-associated autologous chondrocyte transplantation (MACT) of the medial femoral condyle shows a partial delamination (incomplete integration of the anterior cartilage and bone interface) of the MACT (arrow).
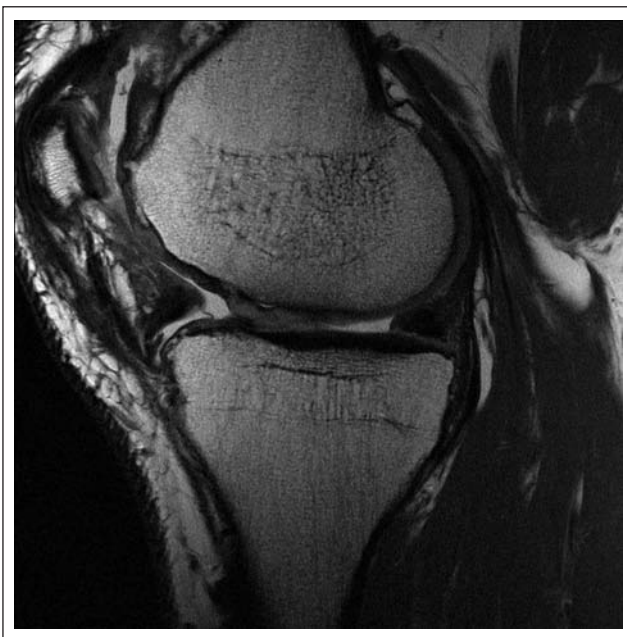
Figure 4. Conventional axial proton density fast spin-echo (PD FSE) sequence (TR/TE: 2400/28) with ultra-high resolution (512 × 512; 12 cm; slice thickness: 2 mm) of a 36-year-old female patient 12 months after matrix-associated autologous chondrocyte transplantation (MACT) of the medial femoral condyle. Moderate hypertrophy of the repair tissue is seen.

that is thicker than the native cartilage and distorts the articular contour (**Fig. 4**). In 5% to 10% of ACI patients, intra-articular adhesions can lead to knee stiffness that requires arthroscopic debridement. Adhesions are most commonly identified in the infrapatellar fat pad, suprapatellar pouch, and parapatellar recesses and appear as thickened bands of intermediate to dark signal tissue extending from the capsule to the articular cartilage or ACI surface. The subchondral bone plate should appear regular on MRI following ACI. The subchondral marrow frequently demonstrates edema-like signal in the early postoperative period, likely a result of the normal healing process. The intensity and volume of the edema-like region tend to diminish over time and regress to normal signal. Persistent or increasing edema-like signal in the marrow beneath an ACI site suggests a problem with the graft or poor integration of the ACI with the subchondral bone and requires close clinical follow-up.[50]

MR Follow-up in Correlation to Clinical Outcome

When looking at the different findings of MR scoring systems, one of the most important variables is the defect fill after cartilage repair techniques. Subdivided into complete, hypertrophy, incomplete >50%, incomplete <50%, and complete delamination, this MOCART variable was shown to correlate to clinical symptoms following matrix-associated autologous chondrocyte transplantation (MACT) by Marlovits et al.[82] In an article by Kreuz et al.,[83] the graft hypertrophy after ACI was further subdivided into 100% to 125% (grade 1), 125% to 150% (grade 2), 150% to 200% (grade 3), and >200% (grade 4). This subdivision correlated with clinical symptoms, with clinical scores worsening with an increasing grade of graft hypertrophy. Furthermore, they showed that surgical intervention for hypertrophy was never necessary for grade 1 and 2 hypertrophy, necessary in 50% of patients with grade 3 hypertrophy, and necessary in all patients with grade 4 hypertrophy.[83]

In a study of the MOCART scoring system, individual variables were correlated with clinical findings as assessed by the visual analog score (VAS) and the Knee Injury and Osteoarthritis Outcome Score (KOOS) for the subgroups of pain, symptoms, activities of daily living (ADL), sports, and knee-related quality of life.[80] In this evaluation, "filling of the defect," "structure of the repair tissue," "changes in the subchondral bone," and "signal intensities of the repair issue" showed a statistically significant correlation with the clinical scores.[82] In a study by Mithoefer et al.,[54] the signal of the repair tissue, the defect fill, the cartilage integration, and possible subchondral edema were analyzed using MRI following microfracture of femoral articular cartilage lesions. The defect fill was correlated with the ADL score, the International Knee Documentation Committee (IKDC) score, and the Short Form-36 physical component score

(SF-36 PCS), and all knees with good fill demonstrated improved knee function, whereas poor fill grade was associated with limited improvement and decreasing functional scores after 24 months. In a study by Henderson et al.,[53] his MR rating system was correlated to IKDC score and the International Cartilage Repair Society (ICRS) knee functional status in patients after ACI. Although improvement in the MR score paralleled the improvement in the IKDC scores for each of the 4 MR variables and the overall score, no significant correlation was established with the clinical scores. In a study after microfracture by Kreuz et al.,[84] the MR rating system of Henderson was performed and correlated to the clinical ICRS score and the Cincinnati knee score. A significant correlation between the clinical scores and the parameter "defect filling" was found. Additional clinical studies correlating the clinical outcome after cartilage repair procedures to MR scores are needed for further validation of the MRI scoring systems. In future validation studies, clinical correlations would ideally determine which morphological or biochemical MR variables have a predictive value and can serve as a surrogate marker for clinical outcome.

Functional (Biochemical) MRI: Clinical Studies

A number of quantitative MRI measurement techniques have been applied to the assessment of the biochemical components of cartilage and cartilage repair tissues. As applied to *in vivo* assessment of cartilage, these measurements require specific acquisitions that generate a series of images, each acquired with different parameters. Using curve fitting programs, the measured values, whether it is T1, T2, or T1rho, are then calculated for the desired regions within the image. The imaging parameters should be carefully chosen to optimize sensitivity for the range of values anticipated within the cartilage or cartilage repair tissues. The number of image data sets acquired, that is, the number of points defining the curve, determines the accuracy of all these measurements and thus the ability to discriminate between values. A trade-off between acquisition time and accuracy of parameter measurement must be made. Validation of the imaging technique with phantoms over the range of expected values should be performed if this has not been previously reported.

dGEMRIC for Assessment of Cartilage Repair

Basic technique. T1 relaxation enhanced by delayed administration of Gd-DTPA^{2-} anion, the dGEMRIC technique, is currently the most widely used method for analyzing PG depletion in articular cartilage and has provided valuable results *in vitro* and *in vivo*.[4,85-88] Glycosaminoglycans (GAGs) are the main source of FCD in cartilage and have

been reported to be lost in the early stage of cartilage degeneration.[89] After IV administration, Gd-DTPA^{2-} penetrates the cartilage through both the articular surface and the subchondral bone. The negatively charged contrast agent equilibrates in inverse relation to the FCD, which is in turn directly related to the GAG concentration. Therefore T1, which is determined by the Gd-DTPA^{2-} concentration, can be used as a specific measure of tissue GAG concentration. An increased accumulation of contrast agent due to a focal depletion of GAG results in lower T1 values in degenerative cartilage regions compared with healthy cartilage. For postcontrast MRI, the dGEMRIC protocol proposed by Burstein et al.[4] is used, that is, application of a bolus of 0.2 mmol Gd-DTPA^{2-} contrast agent per kilogram body weight (double dose). After injection, the patient should moderately exercise the knee, for example, walking up and down stairs for about 20 minutes. Ninety minutes after IV injection, postcontrast MRI should be performed. This delay allows sufficient time for the contrast agent to fully diffuse into the cartilage before the images are acquired. However, because cartilage thickness is variable within the knee and between patients and other joints, the time delay to reach equilibrium should be adjusted to be longer or shorter as appropriate for the joint and cartilage plate to be evaluated.[4] Moreover, the properties of the subchondral bone, in particular after different cartilage repair surgeries, may have an influence on the equilibrium, and the exercise period may be hard to define and standardize.

When evaluating cartilage repair tissue using dGEMRIC, one must take into account that, contrary to studies in normal or degenerative cartilage, the repair tissue may show different T1 values compared with normal cartilage prior to the administration of Gd. Thus, postcontrast T1 mapping may not correlate directly with GAG content, while the difference between precontrast and postcontrast imaging, so-called "delta relaxation rate," $\Delta R1 = 1/T1$ precontrast $- 1/T1(Gd)$, correlates well.[5] Watanabe et al.[5] demonstrated that the relative $\Delta R1$ or "$\Delta R1$ index" (Δ relaxation rate of repair tissue divided by the Δ relaxation rate of normal hyaline cartilage) correlates with the GAG concentration in ACI repair tissue, as measured by gas chromatography, an accepted gold standard for the measurement of GAG content in biopsy samples. However, these results were based on 7 patients, and given the low statistical significance, it is possible that both would show comparable significance with a higher number of samples. In fact, in a recent study, a larger data set of 45 MR examinations in patients after cartilage repair surgery with dGEMRIC technique precontrast and postcontrast T1 mapping revealed a high correlation between the 2 metrics $T1_{Gd}$ and $\Delta R1$ in all examinations with R values above -0.8, even in the separately analyzed patient group in the early postoperative period.[90] The high correlation implies that both metrics yield similar

information. Based on these findings, one can conclude that either parameter might be useful for evaluation of cartilage repair tissue. Because the use of T1(Gd) as the study metric involves only 1 MRI scan instead of 2, the savings in scan time and costs, increased patient compliance, and simplification of the protocol and image processing, it would be desirable to avoid the measurement of ΔR1. If, however, a comparison between the GAG content of native cartilage and repair tissue within the same patient is to be measured, the noncontrast T1 values of the native cartilage and repair tissue need to be similar, or the comparison may not be valid. Further studies are needed to determine if measurement of ΔR1 is necessary for small sample studies and intrapatient comparisons of native and repair cartilage for all types of cartilage repair surgery.

There are many different methods to create T1 parameter maps.[91-96] The methods are based on progressive inversion or saturation of the longitudinal magnetization; in each case, at least 2 data sets with different T1 relevant parameters are required in order to determine the T1 parameter maps. The acquisition times required for T1 maps can be relatively long and often limited to a small number of slice locations. 3-D applications of dGEMRIC that provide greater coverage and faster imaging times are currently undergoing validation.[97-99] A 3-D inversion-recovery prepared spoiled GRE (IR-SPGR) imaging pulse sequence with variable TR has been used to implement a 3-D T1 measurement protocol. T1 measurements in phantoms showed a statistically significant correlation between the 2-D and 3-D measurements at 1.5 T ($R^2 = 0.993$; $P < 0.001$) and 3.0 T ($R^2 = 0.996$; $P < 0.001$). *In vivo* application demonstrated the feasibility of using this 3-D IR-SPGR sequence to evaluate articular cartilage throughout the knee joint with $0.63 \times 0.63 \times 3.0$-mm spatial resolution within a 20-minute acquisition time.[97]

In a recent report, a 3-D T1 mapping sequence at 3.0 T for dGEMRIC based on the Look-Locker scheme has been described, which allows full joint coverage in less than 10 minutes. The sequence employs a magnetization-preparation module prior to data acquisition with a banded k-space data collection scheme.[100] Preliminary data have shown that the 3-D Look-Locker sequence provides accurate T1 values in T1 mapping for dGEMRIC at 3.0 T.[98] Currently, the Look-Locker scheme is a custom sequence and not yet available for widespread use.

A recent study by Trattnig et al.[99] used a 3-D variable flip angle dGEMRIC technique in patients following matrix-induced ACI (MACI) surgery to obtain information related to the long-term development and maturation of grafts within clinically acceptable scan times. This 3-D technique allowed the acquisition of a slab of 36 slices covering a whole compartment of the knee joint with a relatively high resolution, 0.6 mm $\times$ 0.5 mm $\times$ 1.0 mm

(**Fig. 5**). In principle, this sequence can also be used as an isotropic sequence to provide high-resolution reformatting in all planes, without loss of resolution, from one acquisition. Precise registration of precontrast and postcontrast images from the isotropic data set should be possible and further enhance 3-D visualization of the biochemical composition of articular cartilage. As shown in a phantom study, central positioning of the 3-D GRE slab is critical to achieve best results for T1 mapping to eliminate partial volume effects and increase the SNR. When this positioning is performed, a good correlation between variable flip angle technique and standard inversion recovery technique for T1 mapping was shown in phantoms[99] and *in vivo*.[101]

Clinical dGEMRIC studies in patients with cartilage repair. Two studies reported that dGEMRIC has potential as a noninvasive MRI technique for monitoring the GAG content after ACI. The findings of both studies suggest that the GAG concentration in repair cartilage at month 10 (or longer) after ACI[21,102] is comparable with the GAG concentration in the adjacent normal hyaline cartilage. Separately, Trattnig et al.[99] aimed to assess the maturation of cartilage implants in a time-variant cross-sectional study. Biopsy studies have shown that most of the changes in cartilage implants occur in the early postoperative period, and patients were subdivided into an early and late postoperative group (3-13 months and 19-42 months, respectively). The mean ΔR1 (in s^{-1}) for repair tissue was 2.49 ($\pm$1.15) versus 1.04 ($\pm$0.56) at the intact control site in the early postoperative group and 1.90 ($\pm$0.97) compared with 0.81 ($\pm$0.47) in the late postoperative group. The difference in ΔR1 between repair tissue and normal hyaline cartilage was statistically significant ($P < 0.007$) in both groups, but the difference in ΔR1 of repair tissue and normal hyaline cartilage between the groups was not statistically significant ($P = 0.205$). The mean relative ΔR1 was 2.40 in the early group and 2.35 in the late group. A possible explanation for these results comes from histological investigations of biopsies that have shown MACI may develop hyaline-like, mixed hyaline-fibrous, or fibrous tissue over time.[103,104] In a recent longitudinal study of 15 patients with matrix-associated autologous chondrocyte transplantation (MACT), an additional zonal differentiation (analysis of a superficial and deep cartilage layer) was performed. There was a significant difference between the mean ΔR1 of repair tissue and that of reference cartilage at baseline and 1-year follow-up ($P < 0.001$). A significant increase in ΔR1 value and thus a decrease in GAG content from the deep layer to the superficial layer in the reference cartilage and almost no variation and significantly higher values for the repair tissue at both examinations were found. At 1-year follow-up imaging, there was a 22.7% decrease in ΔR1 value in the deep zone of the transplant.[105]

In a study by Kurkijärvi et al.,[21] T2 and dGEMRIC maps were measured in the sagittal and coronal directions in 12 patients 10 to 15 months after ACI. Grafts were assessed for bulk full-thickness, superficial, and deep tissue T2 and dGEMRIC values and were compared with control cartilage. dGEMRIC assessment in the sagittal and coronal directions did not show a significant difference between bulk, superficial, or deep tissue as compared with the control cartilage. Superficial and deep ACI tissue did not differ statistically in terms of their dGEMRIC values.

dGEMRIC has been used to evaluate relative GAG content of repair tissue in patients after different surgical cartilage repair techniques such as microfracture, ACI, and MACI.[21] In one of these studies,[106] 10 patients treated with microfracture and 10 with MACI were compared after being matched by age and postoperative interval. The mean $\Delta R1$ for microfracture was 1.07 ± 0.34 versus 0.32 ± 0.20 at the control site, whereas for MACI, it was 1.90 ± 0.49 versus 0.87 ± 0.44. This resulted in a relative $\Delta R1$ of 3.39 for microfracture and 2.18 for MACI, the difference between the cartilage repair groups being statistically significant. The repair tissue formed by microfracture contained less PGs and an abnormal distribution of collagen compared with normal cartilage (analyzed by histology and biochemistry), which may explain the poor resultant mechanical properties often exhibited by repair tissue.[107,108] These findings are supported by T1 mapping results that showed a significantly higher relative $\Delta R1$ of the repair tissue after microfracture than after MACI, suggesting a lower GAG content after microfracture.

Quantitative MR T1rho

T1rho, or spin-lattice relaxation in the rotating frame, is a time constant that defines the relaxation of spins under the influence of the RF field T1rho. This technique was initially used to investigate slow-motion, low-frequency interactions between hydrogen nuclei in macromolecules and free water.[109] Measurement of T1rho, or T1rho weighting, is acquired by applying spin locking pulses. The spin locking pulse sequence, which is a cluster of RF pulses, starts with a 90° pulse to flip magnetization to the transverse plane, followed by a spin locking pulse along the y axis, "locking" the magnetization into the transverse plane, and a second RF pulse is applied to drive the magnetization back to the z (longitudinal) axis. Initial concerns regarding specific absorption rate (SAR) associated with these special pulses have been addressed through pulse sequence modifications, making them suitable for clinically relevant field strengths at both 1.5 and 3 T.[109,110]

T1rho has been correlated to FCD in both enzymatically degraded bovine and human osteoarthritic explants. In one study, the normalized T1rho rate was strongly correlated with alterations in FCD due to depletion of PG as confirmed by histology.[111] Further, in a porcine model of osteoarthritis induced by the intra-articular injection of recombinant interleukin-1β, subsequent degradation of PG was noted due to the increased expression and activation of matrix metallic proteases.[112] In the latter study, T1rho relaxation rate (1/T1rho) of the treated specimens was noted to have a mean T1rho rate that averaged 25% lower than controls (saline-injected patellae) and a mean reduction of 49% in FCD, as assessed by Na^{23} MRI.[112]

There are preliminary data regarding use of T1rho to assess cartilage repair. Fortier et al. evaluated bone marrow aspirate concentrate as a 1-step arthroscopically applicable method to assess repair of full-thickness cartilage defects in an equine model. Quantitative T1rho and T2 mapping was performed at 3 T as well as histology, including safranin-O/fast green staining and type II collagen immunohistochemistry.[113] The bone marrow aspirate–treated defects had significantly better repair tissue in terms of fill and MR appearance compared with those treated with microfracture alone. T1rho supported the safranin-O/fast green observations with significantly increased GAG content in both the superficial and deep zones within the central and peripheral regions of the bone marrow aspirate–treated tissue as compared with the microfracture-treated control limbs.[113] In the same study, quantitative T2 mapping indicated superior collagen orientation in the superficial and deep zones within the bone marrow aspirate–treated repair tissue compared with the microfracture-treated defects.[113] These data correlated with superior staining for collagen type II immunohistochemistry with the bone marrow aspirate–treated defects. These results indicate that T2 and T1rho mapping provides indirect assessment of the biochemistry of tissue repair.

T2 Mapping

T2 mapping and other techniques that assess collagen provide complementary information to those techniques targeted to PG.[114,115] Quantitative T2 mapping has been shown at both high-field and clinically relevant field strengths to correlate to collagen orientation.[116-119] In native hyaline cartilage, there is a depth-wise variation of T2 relaxation times with shorter T2 values in the deeper, radial zone, where the collagen is highly ordered, and longer values in the transitional zone because of less organization of the collagen. Depending on the pulse sequence parameters, the superficial zone or the lamina splendens may not be visualized on morphological imaging and is too thin to accurately measure relaxation times with quantitative MRI at clinically relevant field strengths.[114]

In the clinical setting, quantitative T2 mapping has been used to detect early degeneration of cartilage in osteoarthritis[120] and may also be used to highlight differences between

immature, disorganized, and more hyaline-like repair tissue. In cartilage repair models, T2 relaxation time has been significantly correlated with collagen orientation using either polarized light microscopy or Fourier transform infrared imaging spectroscopy as standards.[118,119,121] Of note, T2 has a poor correlation with collagen content, showing no significant correlation in several repair models.[121,122]

Several technical details regarding T2 mapping have also been described, including the importance of the stimulated echo contribution that can factitiously elevate T2 values, requiring modification of slice profile to produce more robust T2 measurements.[123] The measurement errors associated with stimulated echo may be avoided by ignoring the first echo acquired in multiecho acquisitions when calculating T2 or by measuring T2 with a series of single echo acquisitions. More efficient T2 data acquisition has been demonstrated with the use of a DESS sequence that has comparable results with the standard multiecho spin-echo T2.[124] However, as with other mapping measurements, the greater the number of data sets, that is, TE values for T2, the greater the accuracy of the T2 measurements. T2 assessment of repair tissue has been described at 1.5-T, 3-T, and 7-T whole body systems as well as high-field (8.5 T) microscopy systems studying repair (**Fig. 6**).[73,118,125-129] Despite the technical challenges of the thinner cartilage of the ankle joint, T2 and T2* assessment of MACT and native cartilage have been described.[130]

Quantitative MR techniques may be used to compare different cartilage repair surgeries, and evaluation may assess either mean global value throughout the thickness of the repair or a zonal assessment in the deep versus the superficial half of the repair tissue. Domayer et al. described a T2 index, defined by the mean global repair tissue T2 divided by the mean global normal cartilage expressed as a percentage; this T2 index correlated with clinical outcome measures including the Lysholm score and the subjective IKDC knee evaluation form.[57] Welsch et al. evaluated 20 patients who underwent either microfracture or MACT with minimum 2-year follow-up.[73] Mean as well as zonal quantitative T2 values were calculated within the repair tissue and morphologically intact native cartilage. The investigators noted that mean T2 was significantly reduced following microfracture but not for MACT, and furthermore, the repair tissue after microfracture showed no significant depth-related zonal variation, whereas MACT showed a significant increase from the deep to the superficial zone, as seen with the intact hyaline cartilage.[73] It is clear that a zonal assessment of repair tissue is optimal, as this will help to discern differences between disorganized repair tissue and the stratified T2 values of intact hyaline cartilage.

Longitudinal evaluation of repair allows for an indirect assessment of the tissue maturation process.[22] Welsch et al. noted stratification in T2 values only after 1 year following MACT; this stratification was not observed at baseline.[131] Similarly, in a phase I Food and Drug Administration (FDA) trial of a tissue-engineered, autologous chondrocyte–seeded collagen scaffold, Crawford et al. noted progressive stratification of T2 values at 24 months in contrast with values obtained at 12-month follow-up.[132]

Quantitative T2 mapping has also been used to assess the interface between transplanted and native cartilage, highlighting immature fibrocartilage and disorganized repair tissue, suggesting a limited ability to produce matrix at the site of peripheral integration. This has been noted in a clinical study of patellar autologous osteochondral transplantation, in which progressive T2 prolongation was noted at the offset of the tidemark that occurred between the thicker native cartilage over the patella and the thinner cartilage over the autologous plug.[126] Similar findings have been described in a canine model comparing autograft with allograft transplantation, where a persistent cleft of disorganized, prolonged T2 tissue was noted at the peripheral integration with the native cartilage, confirmed on subsequent histology.[125]

Quantitative MRI may also provide insight into the comparison of similar cartilage repair techniques performed over different anatomical compartments and thus subject to different contact pressures. Welsch et al. compared T2 mapping of 34 patients treated with MACT over the patella ($N = 17$) versus the medial femoral condyle ($N = 17$), noting prolonged T2 values over the condyle compared with values obtained from the patella repair tissue, indicating differential maturation of the repair tissue as a function of its environment.[133]

Magnetization Transfer Contrast

The use of magnetization transfer (MT) imaging for articular cartilage was first described by Wolff et al.[134] MT effects are based on the interaction of 2 different proton pools, the free (unbound) water pool, which is visible by MRI, and the unseen, very short T2 water pool that is bound to macromolecules. After saturation of the magnetization of bound water molecules by off-resonance or binomial pulses, the equilibrium is shifted to the bound proton pool, which results in a reduction of the observable magnetization and, thus, in a reduction of the MR signal. Thus, MT is specific for tissues with a large number of macromolecules and may provide a quantitative method for tissue characterization of basic macromolecular dynamics and chemistry.[134-139] In the evaluation of articular cartilage, in vitro studies[140,141] show that collagen concentration and collagen orientation may possibly play the most important role for magnetization transfer contrast (MTC). MT has been used for the quantitative in vivo evaluation of articular cartilage, with promising results for cartilage repair (**Fig. 7**).[142,143]
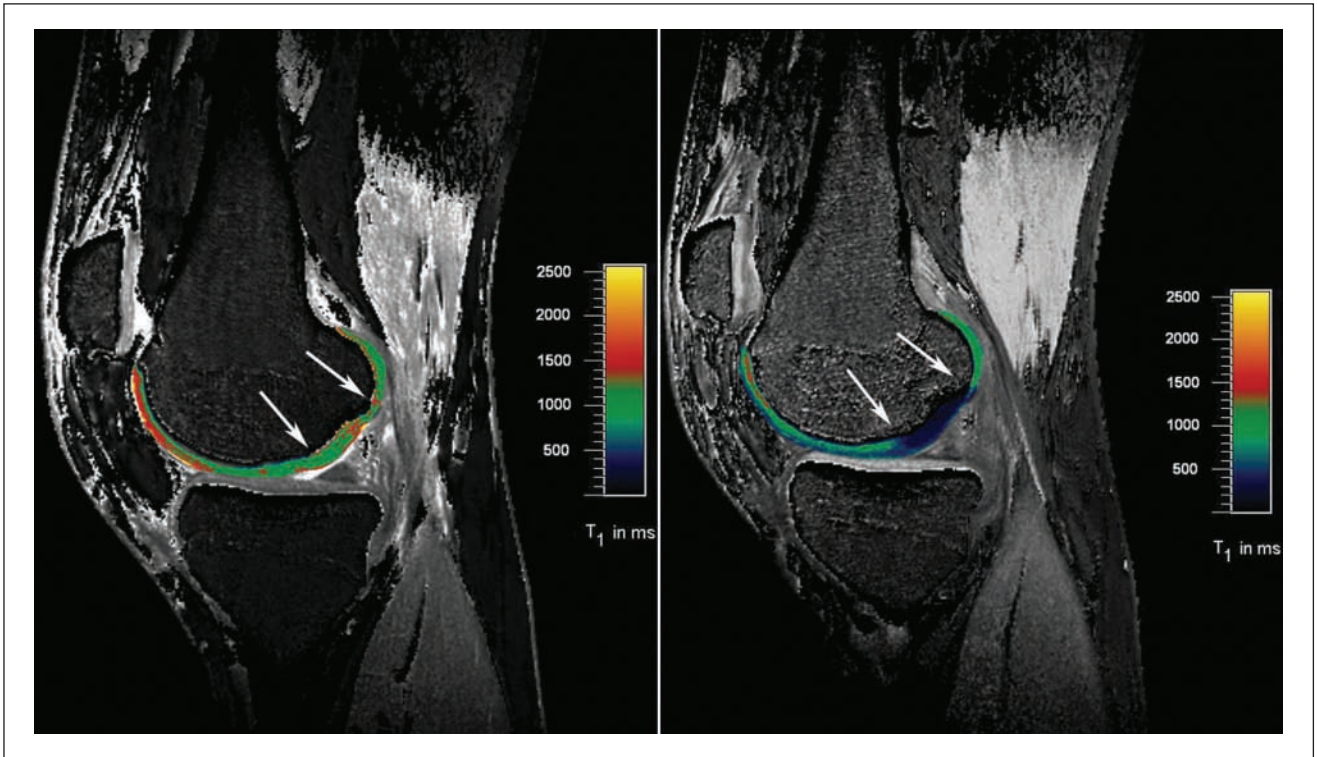
Figure 5. Dual flip angle excitation pulse 3-D gradient-echo (GRE) sequence (TR/TE: 15/3.94) (320 × 320; 16 cm; slice thickness: 3 mm). A flip angle of both 4.6° and 26.1° was used. The acquisition of 22 slices took 1 minute and 53 seconds. The sequence was performed before and after the intravenous application of ionic Gd-DTPA^{2-}. In a 23-year-old male patient 22 months after matrix-associated autologous chondrocyte transplantation (MACT), the repair tissue shows significantly lower T1 values and thus lower glycosaminoglycan (GAG) content compared with normal hyaline cartilage. This is well demonstrated on the postcontrast T1 map but cannot be differentiated on the precontrast T1 map.
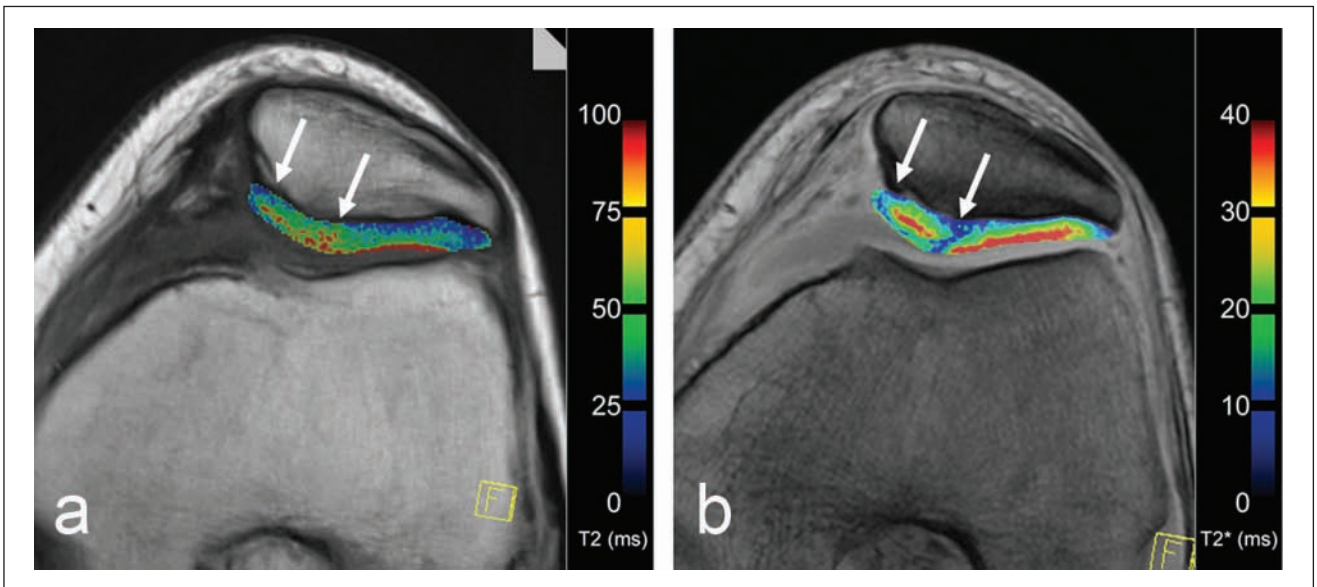
Figure 6. Axial multi-echo (**a**) spin-echo T2 (TR/TE: 1200/12.9, 25.8, 38.7, 51.6, 65.5, 77.4; flip angle: 180°) sequence and (**b**) gradient-echo (GRE) T2* (600/5.7, 9.8, 14.0, 18.1, 22.2, 26.4; flip angle: 20°) sequence with identical high in-plane resolution (384 × 384; 16 cm; slice thickness: 3 mm) visualizing a 29-year-old female patient 24 months after matrix-associated autologous chondrocyte transplantation (MACT) (arrows) within the patella.
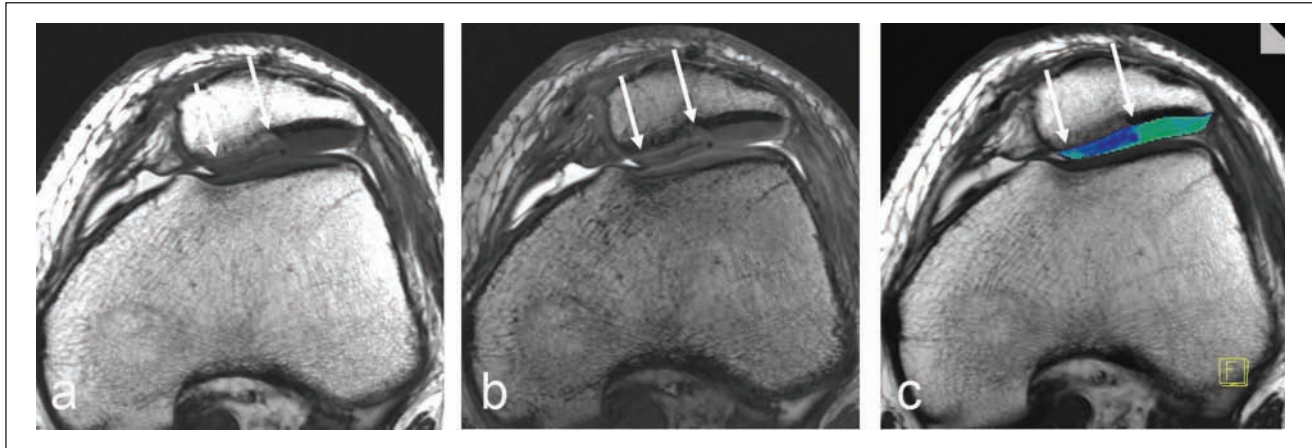
Figure 7. Axial 3-D magnetization transfer (MT)–weighted images of a 17-year-old male patient 3 months after matrix-associated autologous chondrocyte transplantation (MACT) of the patella. MT-saturated (**a**) and MT-free (**b**) images and the corresponding MT contrast (MTC) map (**c**). The MTC map shows clearly lower MTC ratio within the repair tissue (arrows).
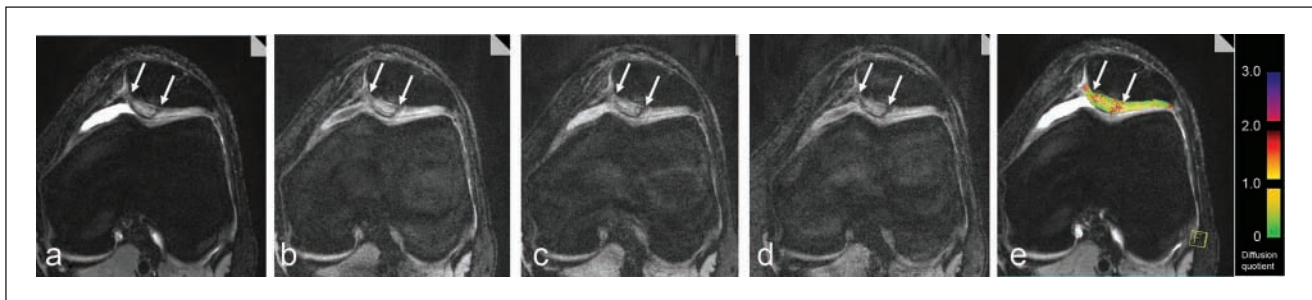
Figure 8. Axial diffusion-weighted images of a patient 24 months after matrix-associated autologous chondrocyte transplantation (MACT) (arrows) of the patella using a high-resolution, 3-D, balanced, steady-state gradient-echo pulse sequence (3-D diffusion-weighted reversed Fast Imaging with Steady State Precession [DW-PSIF]) without (**a**) and with a diffusion gradient of $130 \, T*ms*m^{-1}$ in 3 directions, slice (**b**), phase (**c**), read (**d**), resulting in an apparent diffusion coefficient (ADC) map (**e**) furthermore based on a T1 map and given T2 values. A clearly higher diffusivity of the repair tissue in contrast to the healthy surrounding cartilage is visible.

Twelve months after ACI, a significant difference between the cartilage repair tissue and surrounding control cartilage could be described with an evolution toward normal MT values in the repair tissue after 24 months.[142] In a comparison study between microfracture and MACT using MTC,[143] a new MT-sensitized SSFP approach[144] was prepared providing a fast and signal-intense 3-D MT sequence. MTC and T2 mapping was used in the assessment of global mean values, as well as zonal variations, of articular cartilage and cartilage repair tissue. Compared with T2, MTC showed a similar zonal behavior in its zonal evaluation especially of healthy control cartilage sites. Whereas the differentiation between the repair tissue after microfracture and MACT was better using T2 mapping, MTC showed a better differentiation between healthy cartilage sites and cartilage repair tissue, which is likely due to the more sensitive visualization of collagen structure and content. Very recent MT approaches may base the possibility to gain a

quantification of the free and the bound water in articular cartilage as well as cartilage repair tissue.

Diffusion-Weighted Imaging

Diffusion-weighted imaging (DWI) reflects the self-diffusion of water within tissues. In understanding this image-contrast mechanism, articular cartilage or the repair tissue needs to be considered as a complete system.[145] Basically, DWI is based on molecular motion that is influenced by intracellular and extracellular barriers. Consequently, it is possible to estimate the biochemical structure and architecture of the tissue by measuring molecular movement.[145,146] Echo planar imaging (EPI)–based diffusion sequences are the current gold standard of DWI for neurological applications, however they suffer from limitations in contrast and resolution (due to the long echo times required). These disadvantages render EPI methods very time consuming for

Table 2. Recommendations for Use of Magnetic Resonance Imaging (MRI) in Multicenter Cartilage Repair Trials

Recommendation	Concerns/Variables
Establish imaging core laboratory with expertise in cartilage repair	Allows for standardized and reproducible assessment of RC and compliant registry of patient data
MRI data points (scoring system, pulse sequences, biochemical assessment) in phase I should parallel those used in preclinical models	Preclinical data will allow for relative range of relaxation times and expected morphological appearance of RC
Standardize magnetic field strength	Field strength will affect signal intensity and tissue relaxation times
Standardize imaging coils	Coil design will affect signal-to-noise ratio and image quality
Use cartilage pulse sequence validated for accuracy and reproducibility	MRI treated as an outcome measure
Use published and previously applied morphology assessment system (e.g., MOCART)	MRI treated as an outcome measure
Assess RC fixed charge density (proteoglycan) compared with NC	dGEMRIC; T1rho
Assess RC collagen orientation compared with NC	T2 mapping
Assess zonal (deep, superficial) relaxation times for RC, NC, and tissue at peripheral integration between RC and NC	Provides objective and quantifiable tissue characterization of RC and tissue at peripheral integration with host tissue
Define time points for data collection: 6 months, 1 year, 2 years, etc.	Coordinate MRI metrics with acquisition of subjective clinical outcome instruments
QA concerns: biyearly phantom assessment of relaxation times	Will detect site-specific issues that may lead to inaccuracies in quantitative assessment of RC and NC
Standardize postprocessing algorithm for quantitative assessment	Different algorithms may affect RC and NC relaxation times by up to 20% to 30%

Note: RC = repair cartilage; MOCART = magnetic resonance observation of cartilage repair tissue; NC = native cartilage; dGEMRIC = delayed gadolinium-enhanced MRI of cartilage; QA = quality assurance.

imaging tissues with short T2, such as cartilage and muscle. Alternatively, diffusion imaging can be performed using SSFP sequences, which provide diffusion weighting at relatively short echo times.[147] Zonal evaluation of DWI in articular cartilage is desirable but suffers *in vivo* from the given resolution and signal. However, there are *in vitro* studies that report a zonal pattern of diffusion cartilage imaging[148] as well as a dependency of the diffusivity on the collagen framework.[149] In earlier studies, this reliance on cartilage ultrastructure was evaluated to possibly detect early cartilage matrix damage.[150]

Studies concerning DWI focusing on the SSFP sequence are based on a reversed FISP approach. The so-called 3-D diffusion-weighted reversed Fast Imaging with Steady State Precession (DW-PSIF) sequence is able to provide a semiquantitative assessment of the diffusional behavior of hyaline cartilage and cartilage repair tissue.[61,151,152] Thus, in cartilage repair, the differentiation of the surrounding control cartilage and cartilage repair tissue after MACT is possible because of the higher diffusivity of the repair tissue even years after surgery (**Fig. 8**).[61] In a longitudinal study, nevertheless, the diffusivity seems to decrease over time toward control healthy cartilage.[151] In a multimodal approach, comparing repair tissue after microfracture and MACT, the diffusivity of the repair tissue after microfracture

seems even higher than that after MACT, and an initial correlation with clinical results could be assessed.[152] The feasibility of this technique was also shown in cartilage repair procedures of the thin ankle cartilage.[130] Very recent SSFP DWI sequences provide direct quantification using apparent diffusion coefficient (ADC), which should be the goal for future approaches in the evaluation of cartilage repair procedures.

Part 3: Regulatory Issues
Food and Drug Administration

The current recommendations for the industry in the preparation of investigational device exemption (IDE) or investigational new drug application (IND) for products intended to repair or replace knee cartilage are available on the FDA Web site (http://www.fda.gov). While the document in its current form makes no recommendation for use of noninvasive assessment such as MRI as surrogates for clinically meaningful primary efficacy end points, more recent interest has been raised in the use of MRI in the clinical assessment of cartilage repair (**Table 2**). During a more recent meeting of the Cellular, Tissue and Gene Therapies Advisory Committee (CTGTAC) on May 15,

2009, one of the specific questions posed to the panel was to indicate if substantially new information was available to recommend MRI and/or histological assessments as secondary efficacy end points. Published data were presented and discussed. Clearly, there is an interest in using MRI as an objective assessment of tissue repair; therefore, careful consideration should be given to devising repair trials using MRI as an efficacy end point.

Evaluation of cartilage repair should ideally include both morphological and quantitative imaging. A core laboratory should be established, which will be responsible for collecting the imaging data and phantom assessment, when applicable, storing deidentified patient files in a secure location, and maintaining the technical rigor of the imaging assessment. If the assessment is limited to morphological imaging alone, a standardized protocol should be prepared that uses pulse sequences that have been validated for accuracy in assessing articular cartilage based on the suitable standard such as arthroscopy. In addition, a published record of reproducibility (interobserver/intraobserver variability) using the pulse-specific pulse sequence parameters is recommended. Morphological assessment should be utilized with a published regimen to assess cartilage repair that has been applied to previous cartilage repair studies.[55,153] Standardized score sheets should be used for each study that is interpreted by the core laboratory, detailing the specific features outlined in the scoring system utilized.

Challenges in multi-institutional trials include the use of different field strengths as well as hardware and software from different imaging vendors. It is strongly recommended that an imaging trial be limited to a single field strength, as there is a difference in tissue relaxation times with altering field strength.[154]

In addition, the postprocessing algorithms used to assess quantitative MR parameters vary between vendors and can result in substantial quantitative differences in individual patient data sets. In a longitudinal assessment, a single patient should be evaluated on the same MR system at a consistent field strength. It is recommended that investigators utilizing commercial algorithms to assess quantitative differences request validation data from the vendor, justifying the accuracy of the algorithm in measuring cartilage relaxation times, based on a suitable standard. Standard assessment of tissue relaxation times may be obtained with the use of doped phantoms. These are also recommended to be distributed between sites, with regular interval assessment (ideally, 6 months), in order to maintain quality assurance, both within a single site as well as between sites. Results of phantom data should be compiled at the core laboratory. For example, T2 phantoms set at 30 ms and 60 ms are in standard practice in cartilage repair assessment to reflect the range of T2 values within normal and abnormal cartilage. Intermittent artifacts induced by eddy currents

and white pixel noise may contribute to quantitative MR contamination and may lead to factitious values at clinical assessment. The use of phantoms will therefore alert the core laboratory and, consequently, the individual site for the need for quality assurance with the local field engineer. In addition, equipment upgrades may require phantom calibration evaluations to ensure comparable data. To perform such calibrations, it is necessary to acquire phantom measurements before and after the equipment change; therefore, study coordinators should require clinical sites to inform them of any planned equipment changes before they occur. The choice of imaging coils is also important, as quantitative values may vary between linear, quadrature, or multiple channel phase array coils. As such, standardization of coils for longitudinal assessment is recommended (whenever possible) between sites.

Prior to enrollment of a site for imaging, the selected imaging protocol should be sent and a volunteer patient studied so as to ensure that the morphological images are free of artifact and the quantitative data are within an acceptable range. The site should be able to document a regular schedule of quality assurance (QA) for the MR unit(s), as suggested by the vendor. When the site is enrolled and images are obtained, any deviations from the protocol or issues (such as failure to repeat a sequence for patient motion) should be noted on a standardized QA form. MRI provides a meaningful objective assessment of cartilage repair trial when applied in a thoughtful, rigorous fashion. The selection of the individual sites for imaging should be as careful as the sites chosen for their surgical expertise and patient demographics.

European Medicines Agency (EMEA)

Information about the EMEA's work in the field of advanced therapy medicinal products can be found on their Web site (http://www.emea.europa.eu/htms/human/advanced_therapies/intro.htm). The main document is the "REGULATION (EC) No 1394/2007 OF THE EUROPEAN PARLIAMENT AND OF THE COUNCIL of 13 November 2007 on advanced therapy medicinal products and amending Directive 2001/83/EC and Regulation (EC) No 726/2004." The Committee for Medicinal Products for Human Use (CHMP) has developed a "Guideline on Human Cell-Based Medicinal Products" that came into effect on September 1, 2008. While these documents in their current form make no recommendation for use of noninvasive assessment such as MRI as surrogates for clinically meaningful primary efficacy end points, more recent interest has been raised in the use of MRI in the clinical assessment of cartilage repair as a secondary end point. Therefore, a reflection paper on the role of MRI is in preparation and should be published at the end of 2009.

Recently, the EMEA has recommended the first marketing authorization for an advanced therapy medicinal product, a MACI product, following a positive opinion from the Agency's Committee for Advanced Therapies (CAT) and the CHMP. This first product benefits from the new legal and regulatory framework for advanced therapy medicinal products (Regulation [EC] No 1394/2007). This framework is designed to ensure the free movement of advanced medicines within the European Union (EU), to facilitate their access to the EU market, and to foster the competitiveness of European pharmaceutical companies in the field while guaranteeing the highest level of health protection for patients.

Conclusion

Morphological and biochemical MRI is now possible with high-field MR systems, advanced coil technology, and sophisticated sequence protocols capable of visualizing cartilage repair tissue, the adjacent articular cartilage, and the surrounding structures, *in vivo*, at high resolution, and in clinically applicable scan times. Standard morphological approaches can demonstrate the constitution of cartilage repair tissue. Isotropic 3-D sequences show great promise for improving cartilage imaging and also for the diagnosis of surrounding pathologies within the knee joint. Quantitative/biochemical MR approaches are able to provide a specific measure of the composition of cartilage. Cartilage physiology and ultrastructure can be determined, changes in cartilage macromolecules can be detected, and cartilage repair tissue can thus be assessed and potentially differentiated.

Morphological MRI provides the basis for diagnosis and follow-up evaluation of cartilage defects and surgical cartilage repair, whereas biochemical MRI provides deeper insight into the composition of cartilage and cartilage repair tissue. A combination of both, together with clinical evaluation, may, in the future, represent a desirable multimodal approach to diagnosis as well as for routine clinical follow-up after cartilage repair procedures.

Declaration of Conflicting Interests

Funding

References

1. Gillis A, Gray M, Burstein D. Relaxivity and diffusion of gadolinium agents in cartilage. Magn Reson Med. 2002;48(6):1068-71.

2. Bashir A, Gray ML, Boutin RD, Burstein D. Glycosaminoglycan in articular cartilage: in vivo assessment with delayed Gd(DTPA)(2-)-enhanced MR imaging. Radiology. 1997;205(2):551-8.

3. Dugar A, Farley ML, Wang AL, Goldring MB, Goldring SR, Swaim BH, et al. The effect of paraformaldehyde fixation on the delayed gadolinium-enhanced MRI of cartilage (dGEMRIC) measurement. J Orthop Res. 2009;27(4):536-9.

4. Burstein D, Velyvis J, Scott KT, Stock KW, Kim YJ, Jaramillo D, et al. Protocol issues for delayed Gd(DTPA)(2-)-enhanced MRI: (dGEMRIC) for clinical evaluation of articular cartilage. Magn Reson Med. 2001;45(1):36-41.

5. Watanabe A, Wada Y, Obata T, Ueda T, Tamura M, Ikehira H, et al. Delayed gadolinium-enhanced MR to determine glycosaminoglycan concentration in reparative cartilage after autologous chondrocyte implantation: preliminary results. Radiology. 2006;239(1):201-8.

6. Mow VC, Zhu W, Ratcliffe A. Structure and function of articular cartilage and meniscus. In: Mow VC, Hayes WE, editors. Basic orthopaedic biomechanics. Raven Press, New York: 1991. p. 143-98.

7. Mak AF. The apparent viscoelastic behavior of articular cartilage: the contributions from the intrinsic matrix viscoelasticity and interstitial fluid flows. J Biomech Eng. 1986;108(2):123-30.

8. Korhonen RK, Laasanen MS, Toyras J, Lappalainen R, Helminen HJ, Jurvelin JS. Fibril reinforced poroelastic model predicts specifically mechanical behavior of normal, proteoglycan depleted and collagen degraded articular cartilage. J Biomech. 2003;36(9):1373-9.

9. Nieminen MT, Toyras J, Laasanen MS, Silvennoinen J, Helminen HJ, Jurvelin JS. Prediction of biomechanical properties of articular cartilage with quantitative magnetic resonance imaging. J Biomech. 2004;37(3):321-8.

10. Samosky JT, Burstein D, Grimson WE, Howe R, Martin S, Gray ML. Spatially-localized correlation of dGEMRIC-measured GAG distribution and mechanical stiffness in the human tibial plateau. J Orthop Res. 2005;23(1):93-101.

11. Juras V, Bittsansky M, Majdisova Z, Szomolanyi P, Sulzbacher I, Gabler S, et al. In vitro determination of biomechanical properties of human articular cartilage in osteoarthritis using multiparametric MRI. J Magn Reson. 2009;197(1):40-7.

12. Lammentausta E, Kiviranta P, Nissi MJ, Laasanen MS, Kiviranta I, Nieminen MT, et al. T-2 relaxation time and delayed gadolinium-enhanced MRI of cartilage (dGEMRIC) of human patellar cartilage at 1.5 T and 9.4 T: relationships with tissue mechanical properties. J Orthop Res. 2006;24(3):366-74.

13. Henderson I, Lavigne P, Valenzuela H, Oakes B. Autologous chondrocyte implantation: superior biologic properties of hyaline cartilage repairs. Clin Orthop Relat Res. 2007;455: 253-61.

14. Peterson L, Brittberg M, Kiviranta I, Akerlund EL, Lindahl A. Autologous chondrocyte transplantation: biomechanics and long-term durability. Am J Sports Med. 2002;30(1):2-12.

15. Vasara AI, Nieminen MT, Jurvelin JS, Peterson L, Lindahl A, Kiviranta I. Indentation stiffness of repair tissue after autologous chondrocyte transplantation. Clin Orthop Relat Res. 2005;433:233-42.

16. Grunder W, Wagner M, Werner A. MR-microscopic visualization of anisotropic internal cartilage structures using the magic angle technique. Magn Reson Med. 1998;39(3):376-82.

17. Lusse S, Claassen H, Gehrke T, Hassenpflug J, Schunke M, Heller M, et al. Evaluation of water content by spatially resolved transverse relaxation times of human articular cartilage. Magn Reson Imaging. 2000;18(4):423-30.

18. Fragonas E, Mlynarik V, Jellus V, Micali F, Piras A, Toffanin R, et al. Correlation between biochemical composition and magnetic resonance appearance of articular cartilage. Osteoarthritis Cartilage. 1998;6(1):24-32.

19. Xia Y, Farquhar T, BurtonWurster N, Lust G. Origin of cartilage laminae in MRI. J Magn Reson Imaging. 1997;7(5): 887-94.

20. Nieminen MT, Toyras J, Rieppo J, Hakumaki JM, Silvennoinen J, Helminen HJ, et al. Quantitative MR microscopy of enzymatically degraded articular cartilage. Magn Reson Med. 2000;43(5):676-81.

21. Kurkijarvi JE, Mattila L, Ojala RO, Vasara AI, Jurvelin JS, Kiviranta I, et al. Evaluation of cartilage repair in the distal femur after autologous chondrocyte transplantation using T-2 relaxation time and dGEMRIC. Osteoarthritis Cartilage. 2007;15(4):372-8.

22. Trattnig S, Mamisch TC, Welsch GH, Glaser C, Szomolanyi P, Gebetsroither S, et al. Quantitative T-2 mapping of matrix-associated autologous chondrocyte transplantcation at 3 Tesla: an in vivo cross-sectional study. Invest Radiol. 2007;42(6):442-8.

23. Othman SF, Xu HH, Royston TJ, Magin RL. Microscopic magnetic resonance elastography (mu MRE). Magn Reson Med. 2005;54(3):605-15.

24. Hardy PA, Ridler AC, Chiarot CB, Plewes DB, Henkelman RM. Imaging articular cartilage under compression-cartilage elastography. Magn Reson Med. 2005;53(5):1065-73.

25. Julkunen P, Korhonen RK, Nissi MJ, Jurvelin JS. Mechanical characterization of articular cartilage by combining magnetic resonance imaging and finite-element analysis: a potential functional imaging technique. Phys Med Biol. 2008;53(9):2425-38.

26. Pierce DM, Trobin W, Trattnig S, Bischof H, Holzapfel GA. A phenomenological approach toward patient-specific computational modeling of articular cartilage including collagen fiber tracking. J Biomech Eng. 2009;131(9):091006.

27. Julkunen P, Kiviranta P, Wilson W, Jurvelin JS, Korhonen RK. Characterization of articular cartilage by combining microscopic analysis with a fibril-reinforced finite-element model. J Biomech. 2007;40(8):1862-70.

28. Rubenstein JD, Li JG, Majumdar S, Henkelman RM. Image resolution and signal-to-noise ratio requirements for MR imaging of degenerative cartilage. AJR Am J Roentgenol. 1997;169(4):1089-96.

29. Disler DG, McCauley TR, Kelman CG, Fuchs MD, Ratner LM, Wirth CR, et al. Fat-suppressed three-dimensional spoiled gradient-echo MR imaging of hyaline cartilage defects in the knee: comparison with standard MR imaging and arthroscopy. AJR Am J Roentgenol. 1996;167(1):127-32.

30. Peterfy CG, Vandijke CF, Lu Y, Nguyen A, Connick TJ, Kneeland JB, et al. Quantification of the volume of articular cartilage in the metacarpophalangeal joints of the hand: accuracy and precision of 3-dimensional MR-imaging. AJR Am J Roentgenol. 1995;165(2):371-5.

31. Recht MP, Piraino DW, Paletta GA, Schils JP, Belhobek GH. Accuracy of fat-suppressed three-dimensional spoiled gradient-echo FLASH MR imaging in the detection of patellofemoral articular cartilage abnormalities. Radiology. 1996;198(1):209-12.

32. Recht M, Bobic V, Burstein D, Disler D, Gold G, Gray M, et al. Magnetic resonance imaging of articular cartilage. Clin Orthop Relat Res. 2001;391:S379-96.

33. Potter HG, Linklater JM, Allen AA, Hannafin JA, Haas SB. Magnetic resonance imaging of articular cartilage in the knee: an evaluation with use of fast-spin-echo imaging. J Bone Joint Surg Am. 1998;80(9):1276-84.

34. Trattnig S, Huber M, Breitenseher MJ, Trnka HJ, Rand T, Kaider A, et al. Imaging articular cartilage defects with 3D fat-suppressed echo planar imaging: comparison with conventional 3D fat-suppressed gradient echo sequence and correlation with histology. J Comput Assist Tomogr. 1998;22(1):8-14.

35. Kramer J, Recht MP, Imhof H, Stiglbauer R, Engel A. Postcontrast MR arthrography in assessment of cartilage lesions. J Comput Assist Tomogr. 1994;18(2):218-24.

36. Eckstein F, Sittek H, Milz S, Schulte E, Kiefer B, Reiser M, et al. The potential of magnetic resonance imaging (MRI) for quantifying articular cartilage thickness: a methodological study. Clin Biomech (Bristol, Avon). 1995;10(8):434-40.

37. Eckstein F, Winzheimer M, Westhoff J, Schnier M, Haubner M, Englmeier KH, et al. Quantitative relationships of normal cartilage volumes of the human knee joint: assessment by magnetic resonance imaging. Anat Embryol (Berl). 1998;197(5):383-90.

38. Gray ML, Eckstein F, Peterfy C, Dahlberg L, Kim YJ, Sorensen AG. Toward imaging biomarkers for osteoarthritis. Clin Orthop Relat Res. 2004;427 Suppl:S175-81.

39. Hardy PA, Recht MP, Piraino D, Thomasson D. Optimization of a dual echo in the steady state (DESS) free-precession sequence for imaging cartilage. J Magn Reson Imaging. 1996;6(2): 329-35.

40. Eckstein F, Kunz M, Schutzer M, Hudelmaier M, Jackson RD, Yu J, et al. Two year longitudinal change and test-retest-precision of knee cartilage morphology in a pilot study for the osteoarthritis initiative. Osteoarthritis Cartilage. 2007;15(11):1326-32.

41. Weckbach S, Mendlik T, Horger W, Wagner S, Reiser MF, Glaser C. Quantitative assessment of patellar cartilage volume and thickness at 3.0 Tesla comparing a 3D-fast low angle shot

versus a 3D-true fast imaging with steady-state precession sequence for reproducibility. Invest Radiol. 2006;41(2):189-97.

42. Duc SR, Koch P, Schmid MR, Horger W, Hodler J, Pfirrmann CWA. Diagnosis of articular cartilage abnormalities of the knee: prospective clinical evaluation of a 3D water-excitation true FISP sequence. Radiology. 2007;243(2):475-82.

43. Duc SR, Pfirrmann CWA, Koch PP, Zanetti M, Hodler J. Internal knee derangement assessed with 3-minute three-dimensional isovoxel true FISP MR sequence: preliminary study. Radiology. 2008;246(2):526-35.

44. Duc SR, Pfirrmann CW, Schmid MR, Zanetti M, Koch PP, Kalberer F, et al. Articular cartilage defects detected with 3D water-excitation true FISP: prospective comparison with sequences commonly used for knee imaging. Radiology. 2007;245(1):216-23.

45. Welsch GH, Zak L, Mamisch TC, Resinger C, Marlovits S, Trattnig S. Three-dimensional magnetic resonance observation of cartilage repair tissue (MOCART) score assessed with an isotropic three-dimensional true fast imaging with steady-state procession sequence at 3.0 Tesla. Invest Radiol. 2009;44(9):603-12.

46. Gold GE, Busse RF, Beehler C, Han E, Brau AC, Beatty PJ, et al. Isotropic MRI of the knee with 3D fast spin-echo extended echo-train acquisition (XETA): initial experience. AJR Am J Roentgenol. 2007;188(5):1287-93.

47. Kijowski R, Davis KW, Woods MA, Lindstrom MJ, De Smet AA, Gold GE, et al. Knee joint: comprehensive assessment with 3D isotropic resolution fast spin-echo MR imaging. Diagnostic performance compared with that of conventional MR imaging at 3.0 T. Radiology. 2009;252(2):486-95.

48. Winalski CS, Aliabadi P, Wright RJ, Shortkroff S, Sledge CB, Weissman BN. Enhancement of joint fluid with intravenously administered gadopentetate dimeglumine: technique, rationale, and implications. Radiology. 1993;187(1):179-85.

49. Drape JL, Thelen P, Gay-Depassier P, Silbermann O, Benacerraf R. Intraarticular diffusion of Gd-DOTA after intravenous injection in the knee: MR imaging evaluation. Radiology. 1993;188(1):227-34.

50. Alparslan L, Winalski CS, Boutin RD, Minas T. Postoperative magnetic resonance imaging of articular cartilage repair. Semin Musculoskelet Radiol. 2001;5(4):345-63.

51. Marlovits S, Striessnig G, Resinger CT, Aldrian SM, Vecsei V, Imhof H, et al. Definition of pertinent parameters for the evaluation of articular cartilage repair tissue with high-resolution magnetic resonance imaging. Eur J Radiol. 2004;52(3):310-9.

52. Roberts S, McCall IW, Darby AJ, Menage J, Evans H, Harrison PE, et al. Autologous chondrocyte implantation for cartilage repair: monitoring its success by magnetic resonance imaging and histology. Arthritis Res Ther. 2003;5(1):R60-73.

53. Henderson IJP, Tuy B, Connell D, Oakes B, Hettwer WH. Prospective clinical study of autologous chondrocyte implantation and correlation with MRI at three and 12 months. J Bone Joint Surg Br. 2003;85(7):1060-6.

54. Mithoefer K, Williams RJ, Warren RF, Potter HG, Spock CR, Jones EC, et al. The microfracture technique for the treatment

of articular cartilage lesions in the knee: a prospective cohort study. J Bone Joint Surg Am. 2005;87(9):1911-20.

55. Marlovits S, Singer P, Zeller P, Mandl I, Haller J, Trattnig S. Magnetic resonance observation of cartilage repair tissue (MOCART) for the evaluation of autologous chondrocyte transplantation: determination of interobserver variability and correlation to clinical outcome after 2 years. Eur J Radiol. 2006;57(1):16-23.

56. Choi YS, Potter HG, Chun TJ. MR imaging of cartilage repair in the knee and ankle. Radiographics. 2008;28(4):1043-59.

57. Domayer SE, Kutscha-Lissberg F, Welsch G, Dorotka R, Nehrer S, Gabler C, et al. T2 mapping in the knee after microfracture at 3.0 T: correlation of global T2 values and clinical outcome. Preliminary results. Osteoarthritis Cartilage. 2008;16(8):903-8.

58. Ebert JR, Robertson WB, Lloyd DG, Zheng MH, Wood DJ, Ackland T. Traditional vs accelerated approaches to postoperative rehabilitation following matrix-induced autologous chondrocyte implantation (MACI): comparison of clinical, biomechanical and radiographic outcomes. Osteoarthritis Cartilage. 2008;16(10):1131-40.

59. Henderson I, Gui J, Lavigne P. Autologous chondrocyte implantation: natural history of postimplantation periosteal hypertrophy and effects of repair-site debridement on outcome. Arthroscopy. 2006;22(12):1318-24.

60. Ho YY, Stanley AJ, Hui JH, Wang SC. Postoperative evaluation of the knee after autologous chondrocyte implantation: what radiologists need to know. Radiographics. 2007;27(1):207-20, discussion 221-2.

61. Mamisch TC, Menzel MI, Welsch GH, Bittersohl B, Salomonowitz E, Szomolanyi P, et al. Steady-state diffusion imaging for MR in-vivo evaluation of reparative cartilage after matrix-associated autologous chondrocyte transplantation at 3 Tesla: preliminary results. Eur J Radiol. 2008;65(1):72-9.

62. Marcacci M, Kon E, Delcogliano M, Filardo G, Busacca M, Zaffagnini S. Arthroscopic autologous osteochondral grafting for cartilage defects of the knee: prospective study results at a minimum 7-year follow-up. Am J Sports Med. 2007;35(12):2014-21.

63. Marlovits S. Autologous chondrocyte repair. In: Pietrzak WS, editor. Musculoskeletal tissue regeneration. New York: Humana Press; 2008. p. 369-94.

64. McMahon LA, Reid AJ, Campbell VA, Prendergast PJ. Regulatory effects of mechanical strain on the chondrogenic differentiation of MSCs in a collagen-GAG scaffold: experimental and computational analysis. Ann Biomed Eng. 2008;36(2):185-94.

65. Nettles DL, Kitaoka K, Hanson NA, Flahiff CM, Mata BA, Hsu EW, et al. In situ crosslinking elastin-like polypeptide gels for application to articular cartilage repair in a goat osteochondral defect model. Tissue Eng Part A. 2008;14(7):1133-40.

66. Nemec SF, Marlovits S, Trattnig S. Persistent bone marrow edema after osteochondral autograft transplantation in the knee joint. Eur J Radiol. 2009;71(1):159-63.

67. Robertson WB, Fick D, Wood DJ, Linklater JM, Yheng MH, Avkland TR. MRI and clinical evaluation of collagen/covered autologous chondrocyte implantaion (CACI) at two years. Knee. 2007;14:117-27.

68. Selmi TA, Verdonk P, Chambat P, Dubrana F, Potel JF, Barnouin L, et al. Autologous chondrocyte implantation in a novel alginate-agarose hydrogel: outcome at two years. J Bone Joint Surg Br. 2008;90(5):597-604.

69. Sharma A, Wood LD, Richardson JB, Roberts S, Kuiper NJ. Glycosaminoglycan profiles of repair tissue formed following autologous chondrocyte implantation differ from control cartilage. Arthritis Res Ther. 2007;9(4):R79.

70. Trattnig S, Ba-Ssalamah A, Pinker K, Plank C, Vecsei V, Marlovits S. Matrix-based autologous chondrocyte implantation for cartilage repair: noninvasive monitoring by high-resolution magnetic resonance imaging. Magn Reson Imaging. 2005;23(7):779-87.

71. Trattnig S, Millington SA, Szomolanyi P, Marlovits S. MR imaging of osteochondral grafts and autologous chondrocyte implantation. Eur Radiol. 2007;17(1):103-18.

72. Vanlauwe J, Almqvist F, Bellemans J, Huskin JP, Verdonk R, Victor J. Repair of symptomatic cartilage lesions of the knee: the place of autologous chondrocyte implantation. Acta Orthop Belg. 2007;73(2):145-58.

73. Welsch GH, Mamisch TC, Domayer SE, Dorotka R, Kutscha-Lissberg F, Marlovits S, et al. Cartilage T2 assessment at 3-T MR imaging: in vivo differentiation of normal hyaline cartilage from reparative tissue after two cartilage repair procedures. Initial experience. Radiology. 2008;247(1):154-61.

74. Williams RJ, Brophy RH. Decision making in cartilage repair procedures. In: Williams RJ, editor. Cartilage repair strategies. New York: Humana Press; 2007. p. 37-53.

75. Marlovits S, Mamisch TC, Vekszler G, Resinger C, Trattnig S. Magnetic resonance imaging for diagnosis and assessment of cartilage defect repairs. Injury. 2008;39:S13-25.

76. Berlet GC, Mascia A, Miniaci A. Treatment of unstable osteochondritis dissecans lesions of the knee using autogenous osteochondral grafts (mosaicplasty). Arthroscopy. 1999;15(3):312-6.

77. Lane JM, Brighton CT, Ottens HR, Lipton M. Joint resurfacing in the rabbit using an autologous osteochondral graft. J Bone Joint Surg Am. 1977;59(2):218-22.

78. Dew TL, Martin RA. Functional, radiographic, and histologic assessment of healing of autogenous osteochondral grafts and full-thickness cartilage defects in the talus of dogs. Am J Vet Res. 1992;53(11):2141-52.

79. Pearce SG, Hurtig MB, Clarnette R, Kalra M, Cowan B, Miniaci A. An investigation of 2 techniques for optimizing joint surface congruency using multiple cylindrical osteochondral autografts. Arthroscopy. 2001;17(1):50-5.

80. Minas T, Peterson L. Advanced techniques in autologous chondrocyte transplantation. Clin Sports Med. 1999;18(1):13-44, v-vi.

81. Minas T, Peterson L. Autologous chondrocyte transplantation. Oper Tech Sports Med. 2000;8(2):144-57.

82. Marlovits S, Singer P, Zeller P, Mandl I, Haller J, Trattnig S. Magnetic resonance observation of cartilage repair tissue (MOCART) for the evaluation of autologous chondrocyte transplantation: determination of interobserver variability and correlation to clinical outcome after 2 years. Eur J Radiol. 2006;57(1):16-23.

83. Kreuz PC, Steinwachs M, Erggelet C, Krause SJ, Ossendorf C, Maier D, et al. Classification of graft hypertrophy after autologous chondrocyte implantation of full-thickness chondral defects in the knee. Osteoarthritis Cartilage. 2007;15(12): 1339-47.

84. Kreuz PC, Steinwachs MR, Erggelet C, Krause SJ, Konrad G, Uhl M, et al. Results after microfracture of full-thickness chondral defects in different compartments in the knee. Osteoarthritis Cartilage. 2006;14(11):1119-25.

85. Bashir A, Gray ML, Hartke J, Burstein D. Nondestructive imaging of human cartilage glycosaminoglycan concentration by MRI. Magn Reson Med. 1999;41(5):857-65.

86. Kim YJ, Jaramillo D, Millis MB, Gray ML, Burstein D. Assessment of early osteoarthritis in hip dysplasia with delayed gadolinium-enhanced magnetic resonance imaging of cartilage. J Bone Joint Surg Am. 2003;85(10):1987-92.

87. Tiderius CJ, Olsson LE, Leander P, Ekberg O, Dahlberg L. Delayed gadolinium-enhanced MRI of cartilage (dGEMRIC) in early knee osteoarthritis. Magn Reson Med. 2003;49(3): 488-92.

88. Roos EM, Dahlberg L. Positive effects of moderate exercise on glycosaminoglycan content in knee cartilage: a four-month, randomized, controlled trial in patients at risk of osteoarthritis. Arthritis Rheum. 2005;52(11):3507-14.

89. Lohmander LS. Articular cartilage and osteoarthrosis: the role of molecular markers to monitor breakdown, repair and disease. J Anat. 1994;184(Pt 3):477-92.

90. Trattnig S, Burstein D, Szomolanyi P, Pinker K, Welsch GH, Mamisch TC. T1(Gd) gives comparable information as delta T1 relaxation rate in dGEMRIC evaluation of cartilage repair tissue. Invest Radiol. 2009;44(9):598-602.

91. Homer J, Beevers MS. Driven-equilibrium single-pulse observation of T1 relaxation: a reevaluation of a rapid new method for determining NMR spin-lattice relaxation times. J Magn Reson. 1985;63(2):287-97.

92. Brix G, Schad LR, Deimling M, Lorenz WJ. Fast and precise T1 imaging using a TOMROP sequence. Magn Reson Imaging. 1990;8(4):351-6.

93. Christensen KA, Grant DM, Schulman EM, Walling C. Optimal determination of relaxation times of Fourier-transform nuclear magnetic resonance: determination of spin-lattice relaxation times in chemically polarized species. J Phys Chem. 1974;78(19):1971-7.

94. Deoni SCL, Rutt BK, Peters TM. Rapid combined T-1 and T-2 mapping using gradient recalled acquisition in the steady state. Magn Reson Med. 2003;49(3):515-26.

95. Imran J, Langevin F, Saint-James H. Two-point method for T-2 estimation with optimized gradient-echo sequence. Magn Reson Imaging. 1999;17(9):1347-56.

96. Schmitt P, Griswold MA, Jakob PM, Kotas M, Gulani V, Flentje M, et al. Inversion recovery TrueFISP: quantification of T-1, T-2, and spin density. Magn Reson Med. 2004;52(3):698.

97. McKenzie CA, Williams A, Prasad PV, Burstein D. Three-dimensional delayed gadolinium-enhanced MRI of cartilage (dGEMRIC) at 1.5T and 3.0T. J Magn Reson Imaging. 2006;24(4):928-33.

98. Kimelman T, Vu A, Storey P, McKenzie C, Burstein D, Prasad P. Three-dimensional T1 mapping for dGEMRIC at 3.0 T using the Look Locker method. Invest Radiol. 2006;41(2):198-203.

99. Trattnig S, Marlovits S, Gebetsroither S, Szomolanyi P, Welsch GH, Salomonowitz E, et al. Three-dimensional delayed gadolinium-enhanced MRI of cartilage (dGEMRIC) for in vivo evaluation of reparative cartilage after matrix-associated autologous chondrocyte transplantation at 3.0T: preliminary results. J Magn Reson Imaging. 2007;26(4):974-82.

100. Shah NJ, Zaitsev M, Steinhoff S, Zilles K. A new method for fast multislice T-1 mapping. Neuroimage. 2001;14(5):1175-85.

101. Mamisch TC, Dudda M, Hughes T, Burstein D, Kim YJ. Comparison of delayed gadolinium enhanced MRI of cartilage (dGEMRIC) using inversion recovery and fast T1 mapping sequences. Magn Reson Med. 2008;60(4):768-73.

102. Gillis A, Bashir A, McKeon B, Scheller A, Gray ML, Burstein D. Magnetic resonance imaging of relative glycosaminoglycan distribution in patients with autologous chondrocyte transplants. Invest Radiol. 2001;36(12):743-8.

103. Nehrer S, Minas T. Treatment of articular cartilage defects. Invest Radiol. 2000;35(10):639-46.

104. Tins BJ, McCall IW, Takahashi T, Cassar-Pullicino V, Roberts S, Ashton B, et al. Autologous chondrocyte implantation in knee joint: MR imaging and histologic features at 1-year follow-up. Radiology. 2005;234(2):501-8.

105. Pinker K, Szomolanyi P, Welsch GC, Mamisch TC, Marlovits S, Stadlbauer A, et al. Longitudinal evaluation of cartilage composition of matrix-associated autologous chondrocyte transplants with 3-T delayed gadolinium-enhanced MRI of cartilage. AJR Am J Roentgenol. 2008;191(5):1391-6.

106. Trattnig S, Mamisch TC, Pinker K, Domayer S, Szomolanyi P, Marlovits S, et al. Differentiating normal hyaline cartilage from post-surgical repair tissue using fast gradient echo imaging in delayed gadolinium-enhanced MRI (dGEMRIC) at 3 Tesla. Eur Radiol. 2008;18(6):1251-9.

107. Minas T, Nehrer S. Current concepts in the treatment of articular cartilage defects. Orthopedics. 1997;20(6):525-38.

108. Ghivizzani SC, Oligino TJ, Robbins PD, Evans CH. Cartilage injury and repair. Phys Med Rehabil Clin N Am. 2000;11(2):289-307, vi.

109. Regatte RR, Akella SVS, Wheaton AJ, Borthakur A, Kneeland JB, Reddy R. T-1 rho-relaxation mapping of human femoral-tibial cartilage in vivo. J Magn Reson Imaging. 2003;18(3):336-41.

110. Li X, Benjamin Ma C, Link TM, Castillo DD, Blumenkrantz G, Lozano J, et al. In vivo T(1rho) and T(2) mapping of articular cartilage in osteoarthritis of the knee using 3 T MRI. Osteoarthritis Cartilage. 2007;15(7):789-97.

111. Wheaton AJ, Casey FL, Gougoutas AJ, Dodge GR, Borthakur A, Lonner JH, et al. Correlation of T1rho with fixed charge density in cartilage. J Magn Reson Imaging. 2004;20(3):519-25.

112. Wheaton AJ, Dodge GR, Borthakur A, Kneeland JB, Schumacher HR, Reddy R. Detection of changes in articular cartilage proteoglycan by T(1rho) magnetic resonance imaging. J Orthop Res. 2005;23(1):102-8.

113. Fortier L, Potter HG, Rickey E, Schnabel L, Foo LF, Chong LR. Concentrated bone marrow aspirate improves full-thickness cartilage repair. In: J Bone Joint Surg Am. [In press.]

114. Potter HG, Foo LF. Magnetic resonance imaging of articular cartilage: trauma, degeneration, and repair. Am J Sports Med. 2006;34(4):661-77.

115. Domayer SE, Welsch GH, Nehrer S, Chiari C, Dorotka R, Szomolanyi P, et al. T2 mapping and dGEMRIC after autologous chondrocyte implantation with a fibrin-based scaffold in the knee: preliminary results. Eur J Radiol. 2009 Jan 19 [Epub ahead of print].

116. Xia Y. Heterogeneity of cartilage laminae in MR imaging. J Magn Reson Imaging. 2000;11(6):686-93.

117. Xia Y, Moody JB, Burton-Wurster N, Lust G. Quantitative in situ correlation between microscopic MRI and polarized light microscopy studies of articular cartilage. Osteoarthritis Cartilage. 2001;9(5):393-406.

118. Kelly BT, Potter HG, Deng XH, Pearle AD, Turner AS, Warren RF, et al. Meniscal allograft transplantation in the sheep knee: evaluation of chondroprotective effects. Am J Sports Med. 2006;34(9):1464-77.

119. White LM, Sussman MS, Hurtig M, Probyn L, Tomlinson G, Kandel R. Cartilage T2 assessment: differentiation of normal hyaline cartilage and reparative tissue after arthroscopic cartilage repair in equine subjects. Radiology. 2006;241(2): 407-14.

120. Mosher TJ, Dardzinski BJ, Smith MB. Human articular cartilage: influence of aging and early symptomatic degeneration on the spatial variation of T2. Preliminary findings at 3 T. Radiology. 2000;214(1):259-66.

121. Kim M, Foo L, Lyman S, Ryaby JT, Grande DA, Potter HG, et al. Evaluation of early osteochondral defect repair in a rabbit model utilizing Fourier transform infrared imaging spectroscopy (FT-IRIS), magnetic resonance imaging (MRI) and quantitative T2 mapping. Tissue Eng Part C Methods. 2009 Jul 8 [Epub ahead of print].

122. Watanabe A, Boesch C, Anderson SE, Brehm W, Mainil Varlet P. Ability of dGEMRIC and T2 mapping to evaluate cartilage repair after microfracture: a goat study. Osteoarthritis Cartilage. 2009;17(10):1341-9.

123. Maier CF, Tan SG, Hariharan H, Potter HG. T2 quantitation of articular cartilage at 1.5 T. J Magn Reson Imaging. 2003;17(3):358-64.

124. Welsch GH, Scheffler K, Mamisch TC, Hughes T, Millington S, Deimling M, et al. Rapid estimation of cartilage T2 based on double echo at steady state (DESS) with 3 Tesla. Magn Reson Med. 2009;62(2):544-9.

125. Glenn RE Jr, McCarty EC, Potter HG, Juliao SF, Gordon JD, Spindler KP. Comparison of fresh osteochondral autografts and allografts: a canine model. Am J Sports Med. 2006;34(7):1084-93.

126. Nho SJ, Foo LF, Green DM, Shindle MK, Warren RF, Wickiewicz TL, et al. Magnetic resonance imaging and clinical

evaluation of patellar resurfacing with press-fit osteochondral autograft plugs. Am J Sports Med. 2008;36(6):1101-9.

127. Welsch GH, Mamisch TC, Hughes T, Zilkens C, Quirbach S, Scheffler K, et al. In vivo biochemical 7.0 Tesla magnetic resonance: preliminary results of dGEMRIC, zonal T2, and T2* mapping of articular cartilage. Invest Radiol. 2008;43(9):619-26.

128. Watrin-Pinzano A, Ruaud JP, Cheli Y, Gonord P, Grossin L, Bettembourg-Brault I, et al. Evaluation of cartilage repair tissue after biomaterial implantation in rat patella by using T2 mapping. MAGMA. 2004;17(3-6):219-28.

129. Watrin-Pinzano A, Ruaud JP, Cheli Y, Gonord P, Grossin L, Gillet P, et al. T2 mapping: an efficient MR quantitative technique to evaluate spontaneous cartilage repair in rat patella. Osteoarthritis Cartilage. 2004;12(3):191-200.

130. Quirbach S, Trattnig S, Marlovits S, Zimmermann V, Domayer S, Dorotka R, et al. Initial results of in vivo high-resolution morphological and biochemical cartilage imaging of patients after matrix-associated autologous chondrocyte transplantation (MACT) of the ankle. Skeletal Radiol. 2009;38(8):751-60.

131. Welsch GH, Mamisch TC, Marlovits S, Glaser C, Friedrich K, Hennig FF, et al. Quantitative T2 mapping during follow-up after matrix-associated autologous chondrocyte transplantation (MACT): full-thickness and zonal evaluation to visualize the maturation of cartilage repair tissue. J Orthop Res. 2009;27(7):957-63.

132. Crawford DC, Heveran CM, Cannon WD Jr, Foo LF, Potter HG. An autologous cartilage tissue implant NeoCart for treatment of grade III chondral injury to the distal femur: prospective clinical safety trial at 2 years. Am J Sports Med. 2009;37(7):1334-43.

133. Welsch GH, Mamisch TC, Quirbach S, Zak L, Marlovits S, Trattnig S. Evaluation and comparison of cartilage repair tissue of the patella and medial femoral condyle by using morphological MRI and biochemical zonal T2 mapping. Eur Radiol. 2009;19(5):1253-62.

134. Wolff SD, Chesnick S, Frank JA, Lim KO, Balaban RS. Magnetization transfer contrast: MR imaging of the knee. Radiology. 1991;179(3):623-8.

135. Gray ML, Burstein D, Lesperance LM, Gehrke L. Magnetization transfer in cartilage and its constituent macromolecules. Magn Reson Med. 1995;34(3):319-25.

136. Kim DK, Ceckler TL, Hascall VC, Calabro A, Balaban RS. Analysis of water-macromolecule proton magnetization transfer in articular cartilage. Magn Reson Med. 1993;29(2):211-5.

137. Seo GS, Aoki J, Moriya H, Karakida O, Sone S, Hidaka H, et al. Hyaline cartilage: in vivo and in vitro assessment with magnetization transfer imaging. Radiology. 1996;201(2):525-30.

138. Wolff SD, Balaban RS. Magnetization transfer contrast (MTC) and tissue water proton relaxation in vivo. Magn Reson Med. 1989;10(1):135-44.

139. Wolff SD, Eng J, Balaban RS. Magnetization transfer contrast: method for improving contrast in gradient-recalled-echo images. Radiology. 1991;179(1):133-7.

140. Potter K, Butler JJ, Horton WE, Spencer RGS. Response of engineered cartilage tissue to biochemical agents as studied by proton magnetic resonance microscopy. Arthritis Rheum. 2000;43(7):1580-90.

141. Vahlensieck M, Dombrowski F, Leutner C, Wagner U, Reiser M. Magnetization-transfer contrast (MTC) and MTC subtraction: enhancement of cartilage lesions and intracartilaginous degeneration in-vitro. Skeletal Radiol. 1994; 23(7):535-9.

142. Palmieri F, De Keyzer F, Maes F, Van Breuseghem I. Magnetization transfer analysis of cartilage repair tissue: a preliminary study. Skeletal Radiol. 2006;35(12):903-8.

143. Welsch GH, Trattnig S, Scheffler K, Szomonanyi P, Quirbach S, Marlovits S, et al. Magnetization transfer contrast and T2 mapping in the evaluation of cartilage repair tissue with 3T MRI. J Magn Reson Imaging. 2008;28(4):979-86.

144. Bieri O, Scheffler K. Optimized balanced steady-state free precession magnetization transfer imaging. Magn Reson Med. 2007;58(3):511-8.

145. Miller KL, Hargreaves BA, Gold GE, Pauly JM. Steady-state diffusion-weighted imaging of in vivo knee cartilage. Magn Reson Med. 2004;51(2):394-8.

146. Glaser C. New techniques for cartilage imaging: T2 relaxation time and diffusion-weighted MR imaging. Radiol Clin North Am. 2005;43(4):641-53, vii.

147. Deoni SCL, Peters TM, Rutt BK. Quantitative diffusion imaging with steady-state free precession. Magn Reson Med. 2004;51(2):428-33.

148. Filidoro L, Dietrich O, Weber J, Rauch E, Oerther T, Wick M, et al. High-resolution diffusion tensor imaging of human patellar cartilage: feasibility and preliminary findings. Magn Reson Med. 2005;53(5):993-8.

149. Deng X, Farley M, Nieminen MT, Gray M, Burstein D. Diffusion tensor imaging of native and degenerated human articular cartilage. Magn Reson Imaging. 2007;25(2):168-71.

150. Mlynarik V, Sulzbacher I, Bittsansky M, Fuiko R, Trattnig S. Investigation of apparent diffusion constant as an indicator of early degenerative disease in articular cartilage. J Magn Reson Imaging. 2003;17(4):440-4.

151. Friedrich KM, Mamisch TC, Plank C, Langs G, Marlovits S, Salomonowitz E, et al. Diffusion-weighted imaging for the follow-up of patients after matrix-associated autologous chondrocyte transplantation. Eur J Radiol. 2009 Jan 30 [Epub ahead of print].

152. Welsch GH, Trattnig S, Domayer S, Marlovits S, White LM, Mamisch TC. Multimodal approach in the use of clinical scoring, morphological MRI and biochemical T2-mapping and diffusion-weighted imaging in their ability to assess differences between cartilage repair tissue after microfracture therapy and matrix-associated autologous chondrocyte transplantation: a pilot study. Osteoarthritis Cartilage. 2009;17(9):1219-27.

153. Brown WE, Potter HG, Marx RG, Wickiewicz TL, Warren RF. Magnetic resonance imaging appearance of cartilage repair in the knee. Clin Orthop Relat Res. 2004;422: 214-23.

154. Gold GE, Han E, Stainsby J, Wright G, Brittain J, Beaulieu C. Musculoskeletal MRI at 3.0 T: relaxation times and image contrast. AJR Am J Roentgenol. 2004;183(2):343-51.